

RNI: DELENG/2005/15153
Publication: 23rd of every month
Posting: 27th/28th of every month at DPSO

No: DL(E)-01/5079/2023-25
Licensed to post without pre-payment U(E) 28/2023-25
Rs.150

ISSN 0973-2136

www.mycoordinates.org

Coordinates

Volume XX, Issue 8, August 2024

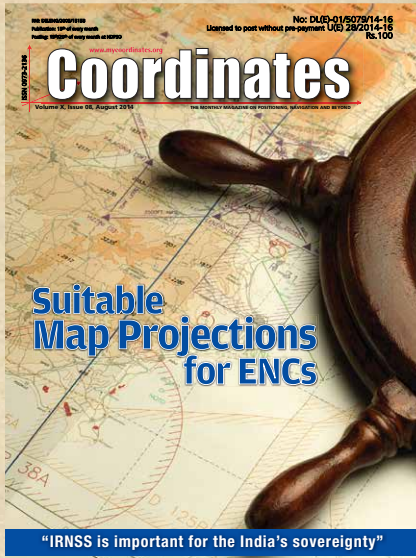
THE MONTHLY MAGAZINE ON POSITIONING, NAVIGATION AND BEYOND

RELIEF PRINTING

INNOVATIVE SOLUTION WITHOUT LIMITING HEIGHTS

Observation of Travelling Ionospheric Disturbances over Morocco

In Coordinates



mycoordinates.org/vol-X-issue-8-August-2014

10 years before...

KOPOS – Kosovo Positioning System

Prof Dr Murat MEHA, Muzafer ÇAKA and Reshat MURATI
Kosovo Cadastral Agency, Prishtina, Republic of Kosovo

KOPOS system in Republic of Kosovo is a unified state reference network which offers in the real-time positioning accuracy in horizontal plane + 2cm and in vertical plane + 4 cm. GNSS system is the latest word of the technology for geodetic measurements, which is used in developed countries. Now as part of the GNSS family is also KOPOS referent network. This system offers the possibility to use the latest technology for geodetic measurements for every surveyor in Republic of Kosovo. GNSS has raised the level of accuracy and reliability of geodetic measurements, because it is a globally extended, secure and with the usage possibility of (American) GPS, (Russian) GLONASS and (European in the future) GALILEO.

Accuracy Assessment of Single-frequency DGPS

Arun Patel, Ravi S Singh, Dr S K Katiyar and Dr Vishnu Prasad

Civil Engineering Department, Maulana Azad National Institute of Technology Bhopal, India

In this study, analysis was done using single frequency DGPS mode of acquiring data such as static and stop-n-go on various baselines.

On high quality Courseware-Making strategies

Erhu WEI and Zhixiang YIN

School of Geodesy and Geomatics, Wuhan University, Wuhan, China

Multimedia teaching can make up for the deficiencies of traditional teaching, which make it rigid, dull and bald. Some innovative projects have been summarized to solve the problems in Courseware-Making in the base of author's teaching experience, and then its validity has been proven by comparing Space Geodesy teaching results. Courseware Making is a systematic work; and the author will master better strategies in future teaching on the basis of students' feedback and self-summary.

Satellite technologies in Turkey

M Cuneyt Bagdatli

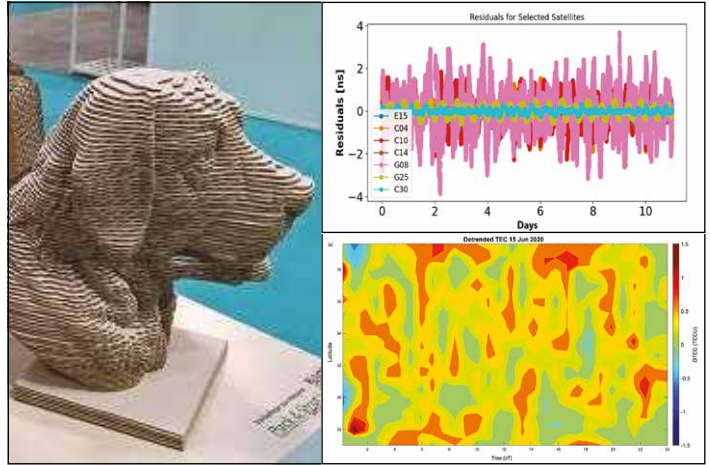
Department of Biosystem Engineering, Engineering and Architecture Faculty, Nevsehir Haci Bektas Veli University, Turkey

This article gives some informations about Satellite Technologies of Turkey called "Yesterday and Today of Developments in Satellite Technologies in Turkey" established by Nevsehir Haci Bektas Veli University, Engineering and Architecture Faculty, Department of Biosystem Engineering.

Performance measurement of EGNOS Integrity and Continuity

H P J Veerman, A J P Van Kleef and J D Van Bruggen van Putten
NLR, Netherlands

This paper addressed the GIMAT EVT and additional methodologies (e.g., bootstrapping) and assessed the results for EGNOS Continuity and Integrity performance with receiver and atmosphere in the loop, based on RIMS observables throughout the entire EGNOS Service Area.



In this issue

Coordinates Volume 20, Issue 8, August 2024

Articles

Observation of travelling ionospheric disturbances over Morocco ULUMA EDWARD, CHALI IDOSA UGA, SOLOMON OTOO LOMOTEY, ATHWART DAVIS ODHIAMBO, FASHAE JOSHUA BANKOLE, KOUASSI NGUESSAN, MUNIAFU WILBERFORCE, BONIFACE NDINYA AND OMONDI GEORGE 5 **GNSS Constellation Specific Monthly Analysis Summary: July 2024** NARAYAN DHITAL 16 **Digital Twins – A panacea for development?** DR SIVA KUMAR RACHAPUDI 20 **Innovative solution for relief printing without limiting heights** FRANÇOIS LECORDIX 24

Columns

Old Coordinates 2 **My Coordinates** EDITORIAL 4 **News** IMAGING 23 GNSS 30 GIS 31 UAV 32 LBS 32 INDUSTRY 33
MARK YOUR CALENDAR 34

This issue has been made possible by the support and good wishes of the following individuals and companies

Athwart Davis Odhiambo, Boniface Ndinya Chali Idosa Uga, Fashae Joshua Bankole, François Lecordix, Kouassi Nguessan, Muniafu Wilberforce, Narayan Dhital, Omondi George, Siva Kumar Rachapudi, Solomon Otoo Lomotey, Uluma Edward; SBG System, and many others.

Mailing Address

A 002, Mansara Apartments
C 9, Vasundhara Enclave
Delhi 110 096, India.
Phones +91 11 42153861, 98102 33422, 98107 24567

Email

[information] talktous@mycoordinates.org
[editorial] bal@mycoordinates.org
[advertising] sam@mycoordinates.org
[subscriptions] iwant@mycoordinates.org
Web www.mycoordinates.org

Coordinates is an initiative of CMPL that aims to broaden the scope of positioning, navigation and related technologies. CMPL does not necessarily subscribe to the views expressed by the authors in this magazine and may not be held liable for any losses caused directly or indirectly due to the information provided herein. © CMPL, 2024. Reprinting with permission is encouraged; contact the editor for details.

Annual subscription (12 issues)
[India] Rs.1,800* [Overseas] US\$100*

*Excluding postage and handling charges

Printed and published by Sanjay Malaviya on behalf of Coordinates Media Pvt Ltd

Published at A 002 Mansara Apartments, Vasundhara Enclave, Delhi 110096, India.

Printed at Thomson Press (India) Ltd, Mathura Road, Faridabad, India

Editor Bal Krishna

Owner Coordinates Media Pvt Ltd (CMPL)

This issue of Coordinates is of 36 pages, including cover.

Observation of Travelling Ionospheric Disturbances over Morocco

We investigate and present results on the propagation characteristics of AGWs associated with the Godzilla SDS event that occurred between 15th and 26th June 2020 over Morocco

Uluma Edward

Department of Physics, Masinde Muliro University of Science & Technology, Kakamega, Kenya

Chali Idosa Uga

Department of Space Science, University of Alabama in Huntsville, Alabama, USA
Department of Physics, Jimma University, Jimma, Oromia, Ethiopia

Solomon Otoo Lomotey

Department of Smart Technologies, University of Environment and Sustainable Development, Somanya, Eastern Region, Ghana

Athwart Davis Odhiambo

Department of Physics, Masinde Muliro University of Science & Technology, Kakamega, Kenya

Fashae Joshua Bankole

Physics Programme, Bowen University, Iwo, Osun State, Nigeria

Kouassi Nguessan

Département de Physique, Université Nangui Abrogoua, Abidjan, Côte d'Ivoire

Muniafu Wilberforce

Department of Physics, Masinde Muliro University of Science & Technology, Kakamega, Kenya

Boniface Ndinya

Department of Physics, Masinde Muliro University of Science & Technology, Kakamega, Kenya

Omondi George

Department of Physics and Materials Science, Maseno University, Maseno, Kenya

Abstract

Using Vertical Total Electron Content (VTEC) data from four GNSS receiver stations: IFR1 (Ifrane Seismic), MELI (Melilla), TETN (Tetouan) and OUCA (Ouca) in Morocco, we investigate the Godzilla sand and dust storm (SDS) event of June 2020 as a source of energetics for generation of travelling ionospheric disturbances (TIDs). Godzilla SDS event began on 5th June 2020 in Algeria following a decrease in pressure and spread to other areas across the Sahara between 6th and 28th June 2020. It was tracked using the Sentinel-5P Satellite mission. Solar wind parameters: Horizontal component of interplanetary magnetic field (IMF Bz), Y-component of interplanetary electric field (IE-Ey), and solar wind speed (Vz) and geomagnetic indices: disturbance storm time (Dst) and planetary K (kp) indices were examined and showed very minimal geomagnetic influence during the period. The study showed that TEC exhibited wave-like structures having distinct troughs and peaks over IFR1-MELI-TETN and OUCA-IFR1-TETN arrays which were clear indicators of generation of TIDs. The arrays and de-trended TEC plots showed that the TIDs propagated poleward. Neutral winds were seen to play a very important role in the propagation of the atmospheric gravity waves (AGWs) which are manifestations of TIDs.

1. Introduction

Travelling ionospheric disturbances (TIDs) are known to be signatures of

atmospheric gravity waves (AGWs) in the ionosphere [1,2]. These wave-like or TID perturbations in the F-layer depend on ionospheric parameters such as wind, electron density and ion temperature [3]. These fluctuations propagate as waves through the ionosphere with wide range of velocities and frequencies. TIDs play an important role in the exchange of energy and momentum between various regions of the upper atmosphere and ionosphere [4]. TIDs and AGWs are related in such a way that TIDs are manifestations of AGWs in the atmosphere [3]. This relationship has been highlighted by various notable studies by Hines, [1,2], Richmond, [5], Hunsucker, [6], Jing & Hunsucker, [7], Hocke & Schlegel, [3]. TIDs are triggered by the ions being forced along the field lines by the neutral air winds driven by the pressure wave [8]. They can also be triggered by geomagnetic or auroral activity, tropospheric activities associated with earthquakes, tsunami, volcanic eruptions, underground nuclear explosions, seismic events, and sand and dust storm (SDS) [4].

Based on their intrinsic properties, TIDs can be categorized either as Large Scale Traveling Ionospheric Disturbances (LSTIDs) or Medium Scale Traveling Ionospheric Disturbances (MSTIDs). LSTIDs have propagation period of 30 minutes to an hour while MSTIDs have propagation period of 15 to 60 minutes. LSTIDs have a wavelength greater than 1000 km and travel with velocities between 300-1000 m/s. MSTIDs have a wavelength of less than 1000 km and travel at a speed of between 100-300 m/s [1,2,5,6,7]. Geomagnetic or aurora activities generate LSTIDs while the lower atmosphere phenomena are a source of MSTIDs [9,10]. When the AGWs propagate vertically upwards from the lower atmosphere carrying energy, they become unstable and start losing energy. However, their amplitude increases due to reduced air density and mechanical friction [11]. MSTIDs have no correlation with geomagnetic activity. They are known to occur during both daytime and nighttime even though the mechanisms of generations causing the daytime and nighttime occurrences vary [12].

Daytime MSTIDs are known to originate from lower or middle atmosphere [13] while nighttime MSTIDs originate from electrodynamical processes which include the Perkins instability, that is associated with the E and F region coupling [14]. The climatology of MSTIDs has a strong dependence on longitude [4]. Tsagouri et al., [4] analyzed LSTIDs based on Digisonde observations over European region over Athens (38°N, 23.5°E), Dourbes (50.1°N, 4.6°N) and Ebre (40.8°N, 0.5°E). They observed a significant uplifting of the F2 layer which corresponded with an oscillation pattern in the foF2 during the LSTID activity. Variations in the height of the peak electron density hmF2 and the corresponding scale height Hm were also observed. However, it was difficult to make conclusion on any sensitivity of the method's results to the electric-field-related disturbances which are common in mid-latitudes zone during geomagnetic storms. Habarulema et al, [14] investigated the storm time equatorward and poleward LSTIDs on global scale. They used total electron content (TEC) observations from GNSS receivers over South American, African and Asian sectors. The results showed the American and African sectors exhibiting predominantly strong poleward TIDs while the Asian sector exhibiting equatorward TIDs which crossed the geomagnetic equator on 9th March 2012. Katamzi & Habarulema, [15] also investigated TIDs over South African latitudes during the 29th to 31st October 2003 which was a geomagnetically disturbed period, using Global Positioning and System (GPS) observations. The results revealed presence of LSTIDs on the days of the geomagnetic storm using line-of-sight vertical TEC measurements from individual satellites. The wave-like structures were seen to propagate equatorward with velocities between 587.04 and 1635.09 m/s.

Sand and dust storm (SDS) events can be sources of energetics that can lead to generation of AGWs which would induce MSTIDs in the ionosphere. The MSTIDs give rise to plasma density gradients as they propagate through the ionosphere

leading to electron density instabilities which manifests as TEC variation [16]. An interesting SDS event known as "Godzilla" SDS which occurred between 1st June and 30th June 2020 across the Sahara Desert was tracked by the Copernicus Sentinel-5P satellite which stores a variety of satellite images used to detect changes in landscape [17] and the offline Satellite Absorbing Index (SAI), which qualitatively shows elevated aerosol layers in atmosphere [18]. The National Oceanic and Atmospheric Administration (NOAA) approximated the Godzilla SDS to be between 60% to 70% larger than the Sand and dust storms experienced in the past [19]. The greatest impact of the Godzilla SDS was felt between 15th and 20th June 2020 [20,21,22].

In the present paper, we investigate and present results on the propagation characteristics of AGWs associated with the Godzilla SDS event that occurred between 15th and 26th June 2020 over Morocco. The study is investigated within geomagnetically quiet period, hence geomagnetic storm-related phenomena is eliminated. We analyze GPS-TEC data from four Global Navigation Satellite System (GNSS) receiver stations situated in Morocco.

2. Materials and methods

2.1 Geomagnetic Indices Data and Solar Wind Parameters

In this study, the periods between 15th and 26th June 2020 were considered due to greatest intensity of the Godzilla SDS event over Morocco [20]. The geophysical conditions such as Kp index showing the level of the geomagnetic activity, the hourly values of Z-component of the interplanetary magnetic field (IMF-Bz), Y-component of the interplanetary electric field (IEFy), solar wind speed (Vz), Planetary K (Kp) and disturbance storm time (Dst) indices were considered during these periods. These parameters were obtained from the archive of OmniWeb website via <https://omniweb.gsfc.nasa.gov/form/dx1>.

2.2 Godzilla SDS Data

The movement of the Godzilla SDS over Morocco was tracked using the Copernicus Sentinel-5P satellite mission which was launched by the European Space agency on 13th October 2017. This satellite uses the Google Earth Engine (GEE), which is a cloud-based platform that stores a variety of satellite images used to detect changes in landscape [23] and the Sentinel-5P Aerosol Index (SAI), which qualitatively shows elevated aerosol layers in atmosphere and the Sentinel-5P Aerosol Index (SAI), which qualitatively shows elevated aerosol layers in atmosphere [18].

2.3 GPS/GNSS Data

The GPS-TEC data were obtained from four GNSS receiver stations in Morocco as shown in the map displayed in Fig. 1 with the station's geographical locations. Table 1 shows the station codes, the station names, geographical and geomagnetic coordinates, and their respective local time. The GPS-TEC data were accessed from the University of NAVSTAR Consortium dual frequency website: <http://unavco.org/data/gps-gnssdata/>.

The GPS-TEC data in the GPS receivers is usually saved in the zipped Receiver Independent Exchange (RINEX) Format which is converted to GPS observable files using appropriate software [24]. In this study, the Gopi software developed by Prof Gopi Krishna Seemala [25] was used to convert the RINEX to observation files. GPS measurements are either code pseudoranges (P) or carrier phases (ϕ). The GPS receiver receives the code time delay and carrier phase difference by cross-correlating the f_1 and f_2 modulated carrier signals, which are normally considered to travel along the same path through the ionosphere [26]. Estimates of GPS-derived ionospheric TEC can be obtained using dual frequency GPS measurements [27,28]. GPS receiver data is critical for estimating the electron density along a ray path between a GPS satellite and a ground receiver [29,30]. Dual-frequency GPS receivers may offer integral information on the ionosphere and plasmasphere. This is done by computing the differential of the code and carrier phase measurements, in addition to removing ionospheric inaccuracies in TEC estimates [31,32]. As a result, the GPS-TEC computed by the dual-frequency receivers is offered as an input to an ionosphere assimilation model [33]. For the present study, GPS-TEC data collected in dual-frequency receivers was used. The GPS-TEC data was obtained using the pseudo-range and carrier phase measurements. The TEC calculated from the pseudo-range measurement (slant TEC) is given by Equation 1:

$$STEC = \frac{1}{40.3} \left[\frac{f_1^2 f_2^2}{f_1^2 - f_2^2} \right] (P_2 - P_1) \quad (1)$$

Similarly, the TEC from carrier phase measurement may be calculated as follows using Equation 2:

$$STEC = \frac{1}{40.3} \left[\frac{f_1^2 f_2^2}{f_1^2 - f_2^2} \right] (\phi_2 - \phi_1) \quad (2)$$

where f_1 and f_2 are GPS satellite frequencies determined from the fundamental frequency, $f_o = 10.23$ MHz as: ($f_1 = 154$, $f_o = 1,575.42$ MHz, ($f_2 = 120$, $f_o = 1,227.60$ MHz), and the differential code and phase measurements are ($P_2 - P_1$) and ($\phi_1 - \phi_2$), respectively [34]. The vertical total electron content (VTEC) is obtained using the relations in Equation 3:

$$VTEC = STEC \times \cos(\chi') \quad (3)$$

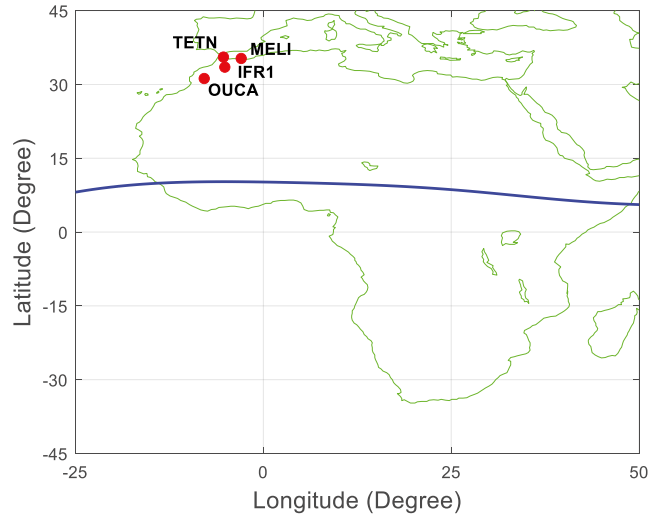


Fig. 1. Geographic locations of the the four GNSS receiver stations over Morocco

where the zenith angle χ' is given by Equation 4:

$$\chi' = \arcsin \left[\frac{R_E \cos \alpha}{R_E + h} \sin(\chi) \right] \quad (4)$$

VTEC is therefore given by equation 5:

$$VTEC = STEC \left\{ \cos \left[\arcsin \left(\frac{R_E \cos \alpha}{R_E + h} \right) \sin(\chi) \right] \right\} \quad (5)$$

Where α is the satellite's elevation angle, R_E is the Earth's mean radius, and h is the height of the ionospheric layer, which is considered to be 400 km.

To reduce multipath effects, the data selected was for elevation angles of 30° and above [35]. This was to eliminate multipath errors.

Information for the four GNSS receiver stations: MELI, IFR1, OUCA and TETN is given in Table 1.

The average of VTEC for all PRNs for IFR1, MELI, OUCA and TETN during study period were obtained by averaging the VTEC values for all identical pseudo-random numbers (PRNs) within a 24 hour period [36] and used to plot VTEC against Universal Time (UT) for each day and station. The VTEC against universal time (UT) plots for each day were analyzed.

2.4 Methodology

2.4.1 Extracting travelling Ionospheric disturbances (TIDs) from GPS-TEC data

Background or unperturbed ionospheric TEC was determined by fitting each satellite's time series of the VTEC data with a fourth polynomial across all the four GNSS receiver stations. This was done using equation 6.

$$VTEC_{fit} = at_{ij}^4 + bt_{ij}^3 + ct_{ij}^2 + dt_{ij} + \epsilon \quad (6)$$

where $VTEC_{fit}$ is fitted VTEC at time t , $i = 1, 2, 3, 4$. (No of receiver stations), $j = 1, 2, \dots, 32$ (the number of satellites), ϵ is the residual error of the fitting process and coefficients a , b , c and d are obtained using least squares method [14].

High frequency changes in $\Delta VTEC$ due to irregular ionospheric plasma was detected by finding the difference between actual VTEC data and modeled data using equation 7.

$$\Delta VTEC = VTEC - VTEC_{fit} \quad (7)$$

Where, $\Delta VTEC$ = deviation of VTEC $VTEC$ = actual VTEC data at time t $VTEC_{fit}$ = modeled data

$\Delta VTEC$ gives information about the spectral content of the signal and how it changes with time. Plots of VTEC versus UT were plotted alongside their corresponding $\Delta VTEC$ versus UT plots. The potential wavelike structures were monitored across the across three stations along close latitudes. In this case, two receiver arrays were considered: OUCA-IFR1-TETN and the IFR1- MELI-TETN receiver arrays. The amplitudes of the wavelike structures (TIDs) that modulate TEC were inferred by monitoring $\Delta VTEC$ [14,37].

Detrended TEC from GPS-TEC data was created using the Savitzky-Golay filter with a 60-minute sliding window for all the four GNSS receiver stations and visible satellites [38]. The Savitzky-Golay filter uses quadratic polynomial that is fitted over each sliding window. The detrended TEC over all geographic latitudes against Universal time (UT) were directly constructed in a temporal resolution of 10 minutes. The derived detrended TEC plots along geographical latitudes were then used to investigate propagation behavior of the Godzilla SDS induced TIDs [39].

3. Results and discussion

3.1 The Movement of the Godzilla SDS between 15th and 26th June 2020 over Sahara

The movement of the Godzilla SDS over Morocco between 15th and 26th June 2020 was tracked using the Copernicus Sentinel-5P satellite. During the study period, the Western part of Africa such as Mauritania, Mali, Morocco and Western Sahara felt the greatest impact of the Godzilla SDS [2] as in 2 and 3. By 20th June 2020, the first traces of dust had reached the Caribbean [40]. Large SDS traces were observed over the upper parts of the Sahara between 21st June and 26th June 2020 as shown in Fig. 3.

In Figs. 2 and 3, the cream colour on the SAI indicates low aerosol concentrations in the atmosphere while red colour shows presence of high aerosol concentrations in the atmosphere during the Godzilla SDS of June 2020 as tracked by the Copernicus Sentinel-5P satellite.

3.2 The Variation of Solar Wind Parameters between 15th and 26th June 2020

Fig. 4 depicts the changes in IMF Bz, IEF Ey, the solar wind speed, kp and Dst indices between 15th and 26th June 2020.

Noted that from Fig. 4, on 15th June 2020, there was a southward turning of the IMF-Bz of -3 nT with a corresponding rise of IEF-Ey of 1. The solar wind speed rose to maximum, of 330 km/s. The highest kp index value of 1.5 and lowest Dst value of -8 nT were attained. On 16th June 2020, the southward turning of -2.5 nT was attained with a corresponding rise in IEF-Ey of 1.5. The lowest solar wind speed of 280 km/s was attained. The maximum kp index value attained was 2.2 with minimum Dst value of -11 nT. On 17th and 18th June 2020 there was a southward turning of -5 nT with a corresponding IEF-Ey of 1. The solar wind speed dropped from 320 km/s to 280 km/s on 17th June and rose to a maximum of 320 km/s on 18th June 2020. The maximum Dst value of 1.8 nT was attained on 17th and 18th June with a corresponding Dst value of -10 nT. On 20th June 2020, the IMF-Bz southern turning reached -6 nT with a corresponding IEF-Ey value of 2. This corresponded well with a solar wind speed of 350km/s. Between 15th and 26th June 2020, the highest Kp value of 2.2 was attained with a corresponding Dst index value of -11 nT on 19th June 2020. The solar wind parameter shows a minimum solar wind speed of 270 km/s on 16th June 2020 and

Table 1. Information of the geographical and geomagnetic locations of the stations over Morocco

Station code	Station Name	Geographic Latitude	Geographic Longitude	Geomagnetic Latitude	Geomagnetic Longitude	Local Time
MELI	Melilla	35.28°N	2.95°W	25.64°N	77.44°W	UT+1
IFR1	Ifrane Seismic	33.52°N	5.13°W	23.14°N	79.03°W	UT+1
OUCA	Ouca	31.206°N	7.87°W	20.04°N	81.12°W	UT+1
TETN	Tetouan	35.56°N	5.36°W	26.15°N	79.51°W	UT+1

maximum solar wind of 360 km/s on 20th June 2020. During solar minimum, solar wind of speeds between 250 km/s and 400 km/s originates from regions close to the heliospheric current sheet at the heliomagnetic equator while the fast solar wind having speeds of between 400 km/s and 800 km/s which originates from coronal holes when the magnetic field is open [41]. The solar wind parameters and geomagnetic indices in Fig. 4 indicate a very minimal geomagnetic field influence on the ionosphere between 15th and 26th June 2020.

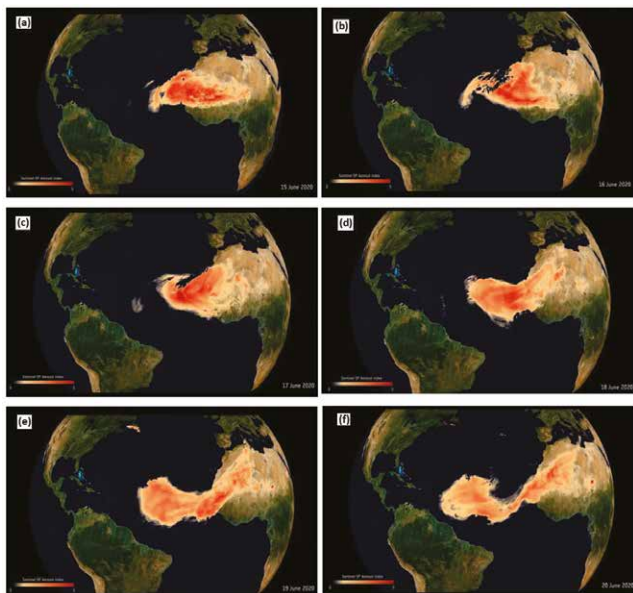


Fig. 2. The Copernicus Sentinel-5P satellite images of Godzilla SDS over the Sahara for (a) 15.06.2020 (b) 16.06.2020 (c) 17.06.2020 (d) 18.06.2020 (e) 19.06.2020 (f) 20.06.2020 (European space Agency, 2020)

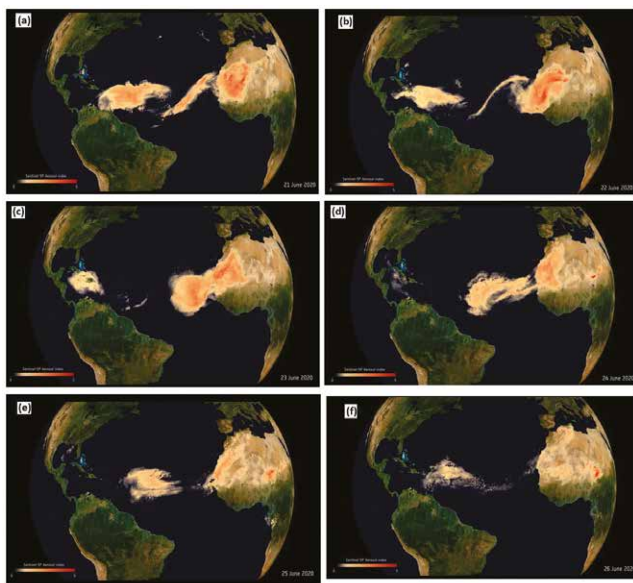


Fig. 3. The Copernicus Sentinel-5P satellite images of Godzilla SDS over the Sahara for (a) 21.06.2020 (b) 22.06.2020 (c) 23.06.2020 (d) 24.06.2020 (e) 25.06.2020 (f) 26.06.2020 (European space Agency, 2020)

3.3 Variations of TEC and VTEC_{fit} against UT

Figs. 5 and 6 show the VTEC and VTEC_{fit} against UT for OUCA-IFR1-TETN receiver array while Figs. 7 and 8 shows the VTEC and VTEC_{fit} against UT for IFR1- MELI-TETN receiver array between 15th and 26th June 2020 respectively.

3.3.1 OUCA-IFR1-TETN receiver array

Based on Figs. 5 and 6, on 15th, 23rd and 24th June 2020 triple peak structures (indicated by black arrows) were observed between 7:00 and 21:00 UT with the first peak appearing approximately at 08:00 UT, the second peak appearing approximately at 16:00 UT, while the third peak appearing approximately at 20:00 UT. From 16th to 20th June 2020, double peak structures were observed between 07:00 and 12:00 UT with the first peak appearing approximately at 08:00 UT and the second peak appearing approximately at 20:00 UT. On 16th, 17th, 18th, 19th, 21st, 22nd, 25th and 26th June 2020, double peak structures however were observed between 7:00 and 12:00 UT with the first peak appearing approximately at 08:00 UT and the second peak appearing approximately at 20:00 UT.

3.3.2 IFR1-MELI-TETN receiver array

Based on Figs. 7 and 8, it was also noted that on 15th, 23rd and 24th June 2020, triple peak structures were observed between 7:00 and 21:00 UT with the first peak appearing approximately at 08:00 UT, the second peak appearing approximately at 16:00 UT while the third peak appearing approximately at 20:00 UT Double peaks were observed on 16th, 17th, 18th, 19th, 20th, 21st, 22nd, 25th

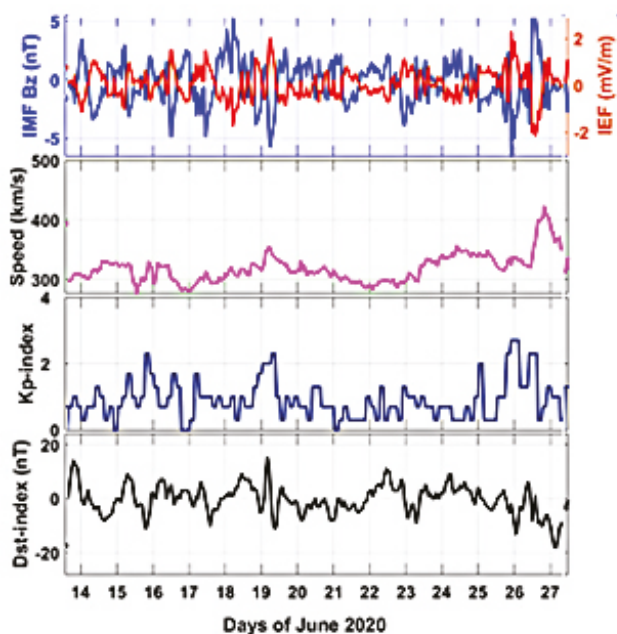


Fig. 4. Variations of Solar wind parameters; IMF-Bz, IEF-Ey and the solar wind speed and the geomagnetic indices; kp and Dst index, between 15th and 26th June 2020

and 26th June 2020 with the first peak appearing approximately at 10:00 UT, the third peak appearing approximately at 18:00 UT. A close analysis of Figs. 5, 6, 7 and 8 showed that the two receiver arrays exhibited similar wave-like structures. The peaks were observed to all appear between 7:00 and 12:00UT after sunrise and between 18:00 and 21:00UT after sunset.

It was also noted that the two receiver arrays show peak structures for the lower latitude stations (OUCA and IFR1) being

observed first as compared to the other receiver stations. This indicates that there was a pole-ward propagation of the TIDs.

3.4 Changes in Detrended TEC (Δ TEC)

Figs. 9 to 14 show plots of detrended TEC along geographic latitude against UT for the four GNSS receiver stations between 15th and 26th June 2020.

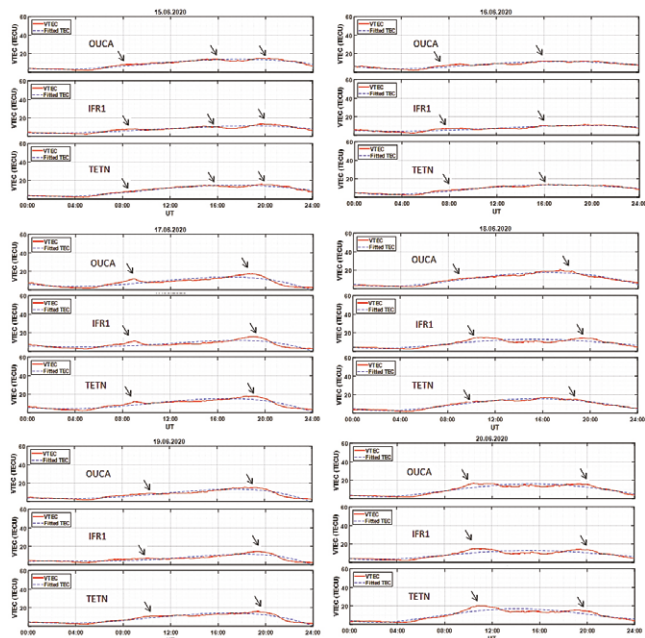


Fig. 5. VTEC and VTECfit against UT for OUCA-IFR1-TETN receiver array between 15th- 20th June 2020

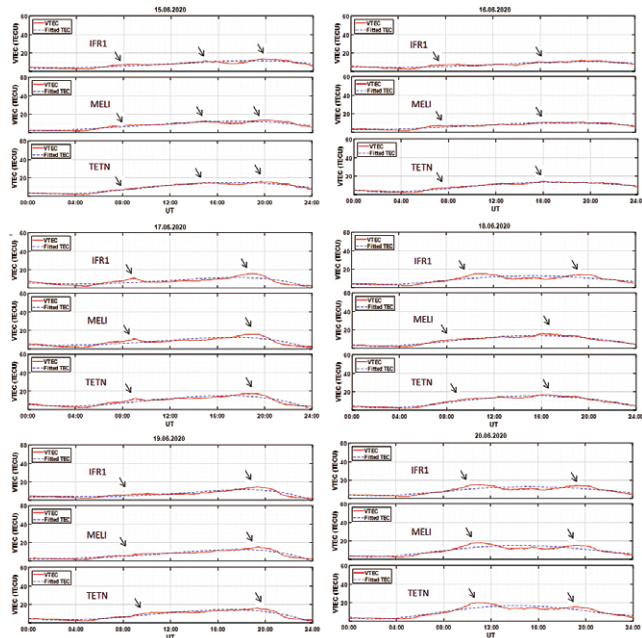


Fig. 7. VTEC and VTECfit against UT for IFR1-MELI-TETN receiver array between 15th- 20th June 2020

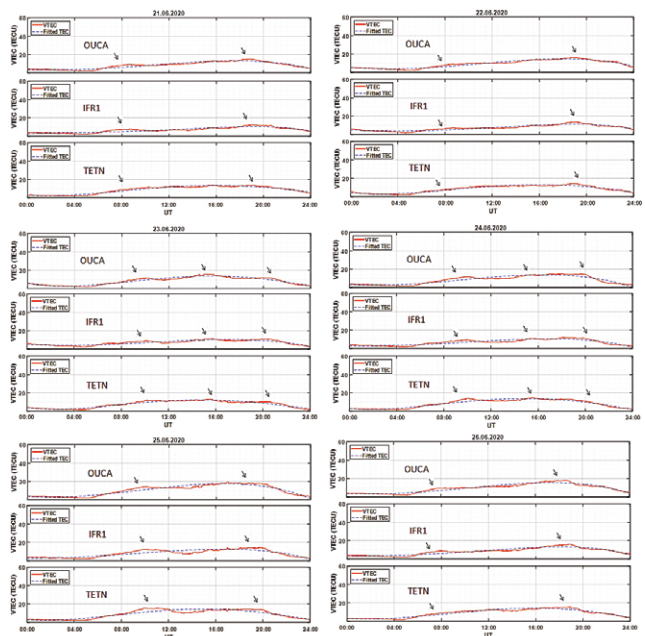


Fig. 6. VTEC and VTECfit against UT for OUCA-IFR1-TETN receiver array between 21st-26th June 2020

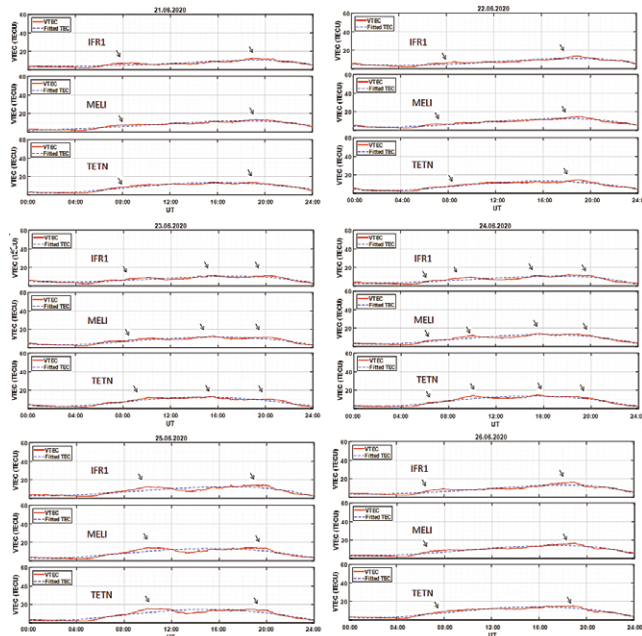


Fig. 8. VTEC and VTECfit against UT for IFR1-MELI-TETN receiver array between 21st- 26th June 2020

In these Figures, band structures were observed over the 24-hour period for all the days between 15th and 26th June 2020. In Figs. 9(a), 9(b), 11(b), 12(a) and 12(b) the band structures for DTEC ranged between 0.5 and 1.0 TECU. In Figs. 10(a), 10(b), 11(a), 13(a), 13(b) the band structures for DTEC ranged

between 0.6 and 1.5 TECU. In Figs. 14(a) and 14(b), the band structures for DTEC ranged between 0.5 and 1.2 TECU.

In Figs. 9 - 14, we can observe evident poleward propagating band structures during the 24-hour period for all the days

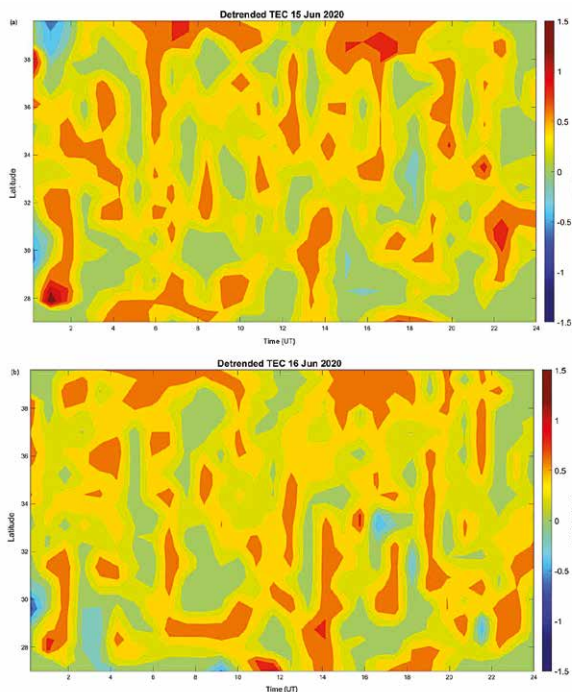


Fig. 9. Plot of detrended TEC along geographic latitudes against UT for: (a) 15.06.2020, (b) 16.06.2020

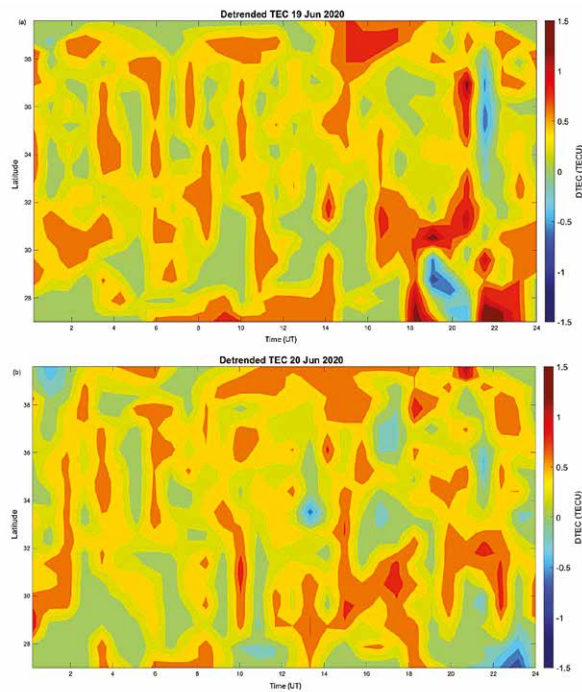


Fig. 11. Plot of detrended TEC along geographic latitudes against UT for: (a) 19.06.2020 (b) 20.06.2020

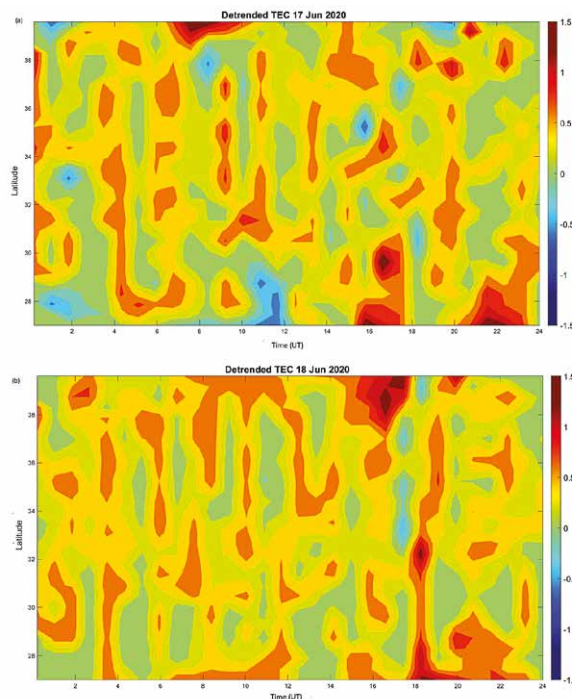


Fig. 10. Plot of detrended TEC along geographic latitudes against UT for: (a) 17.06.2020 (b) 18.06.2020

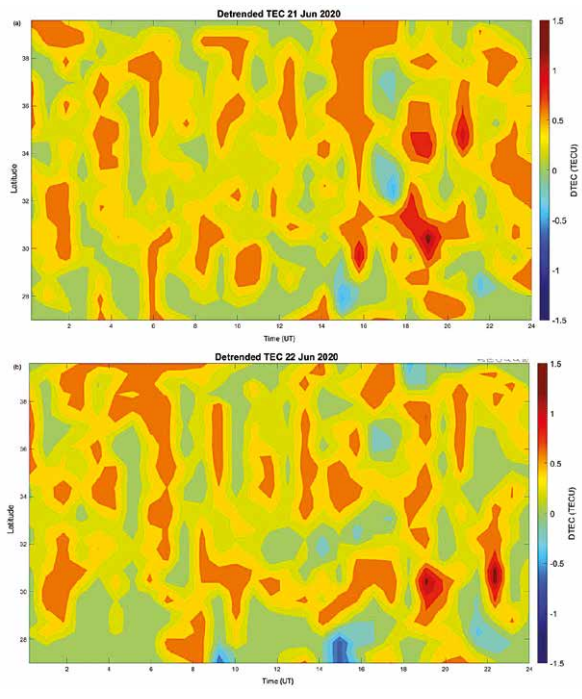


Fig. 12. Plot of detrended TEC along geographic latitudes against UT for: (a) 21.06.2020 (b) 22.06.2020

between 15th and 26th June 2020. The band structures depicts present of TIDs. We also observe important values of detrended DTEC at the time of VTEC peaks. For example, Figs. 10(a) and 11(a) show DTEC values of above 1 when VTEC has the large peaks around 18:00 UT. The band structures depict presence of TIDs that is important when VTEC is maximum.

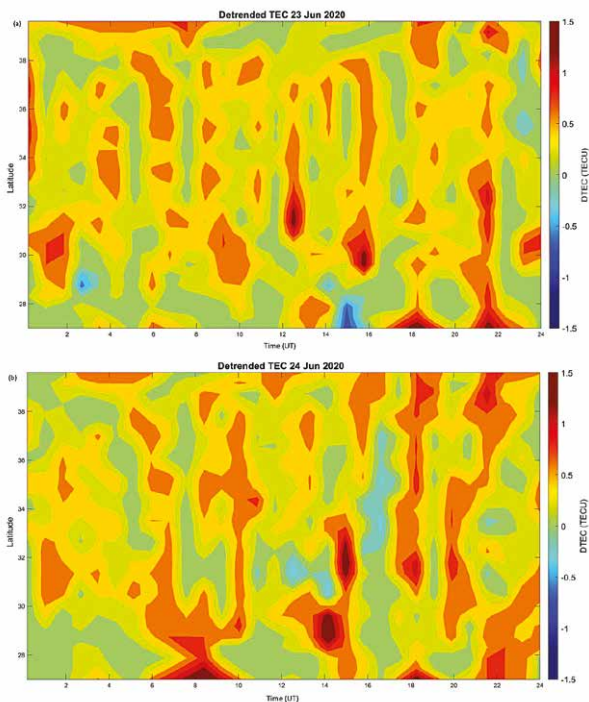


Fig. 13. Plot of detrended TEC along geographic latitudes against UT for: (a) 23.06.2020 (b) 24.06.2020

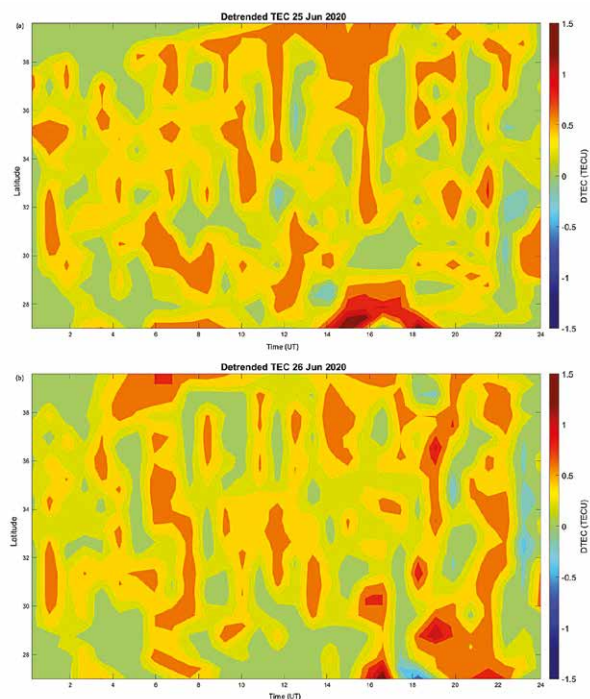


Fig. 14. Plot of detrended TEC along geographic latitudes against UT for: (a) 25.06.2020 (b) 26.06.2020

The present study successfully demonstrates that SDS events are a source of energetics for generation of TIDs which are signatures of AGWs. The Dst and kp indices in Fig. 4 rule out the influence of geomagnetic activity in the generation of TIDs. Therefore, the TEC results from this study exclude the effect of geomagnetic disturbances but are fully attributed to the effect of the SDS. During SDS events, internal waves are continuously generated and breaking throughout the atmosphere [11]. Wave breaking effectively mixes sand and dust aerosols through the atmosphere and contributes to driving some larger-scale flows. The gravity waves (GWs) generated are affected by the changing stratification as they propagate. Each of these interactions, in addition to gravity wave dissipation, may contribute to the vertical flux of horizontal momentum and the universal frequency spectrum in the middle atmosphere [42,43,44,45]. The possible cause of these types of disturbances is the neutral winds [46]. Neutral winds play an important role in the wave breaking/dissipation in the mesosphere and lower thermosphere to global redistribution of energy and momentum deposited at high latitudes by the magnetosphere [47]. They are usually slower than the actual wind in stable conditions and faster in unstable conditions i.e. land surface or sea stress. When GWs propagate into the ionosphere, the measured TEC exhibits clear wavelike-structures, as shown in Figs. 5, 6, 7 and 8. Their peaks and troughs are imaged on the ionospheric pierce points (IPP) trajectory at different moments and different propagation distances. This makes observation of GWs propagation possible.

4. Conclusion

We have investigated the generation of TIDs during the Godzilla SDS event of June 2020 over Morocco using GPS-TEC data. The obtained results showed TEC exhibited wave-like structures having distinct troughs and peaks over IFR1-MELI-TETN and OUCA-IFR1-TETN arrays which were clear indicators of generation of TIDs. The arrays showed that the TIDs propagated poleward (along latitude). This was supported by the evident poleward propagating band structures on the detrended TEC plots during the 24-hour period for all the days between 15th and 26th June 2020. The band structures on the plots also depicted the presence of TIDs. Neutral winds were seen to play a very important role in the propagation of the AGWs which are manifestations of TIDs. In conclusion, the study confirms that SDS events can be a source of energetics for the generation of MSTIDs.

Disclaimer (Artificial Intelligence)

Author(s) hereby declare that NO generative AI technologies such as Large Language Models (ChatGPT, COPILOT, etc) and text-to-image generators have been used during writing or editing of manuscripts.

Acknowledgements

The authors thank the University of NAVSTAR Consortium: <http://unavco.org/data/gps-gnssdata/> for the GNSS data; Kyoto: wdc.kugi.kyoto-u.ac.jp/dst/index.html and Kyoto: www.kugi.kyoto-u.ac.jp/kp for the geomagnetic activity data; <https://omniweb.gsfc.nasa.gov/form/dx1.html> for the daily values of solar wind parameters and the European Space Agency for the Copernicus Sentinel-5P satellite images of June 2020 Godzilla SDS over the Sahara. They also thank Prof Gopi Seemala of the Indian Institute of Geomagnetism for the GPS-TEC analysis software.

Competing interests

Authors have declared that no competing interests exist.

References

- Hines CO. Internal atmospheric gravity waves at ionospheric heights. *Can. J Phys.* 1960;38:1414.
- Hines CO. The upper atmosphere in motion, Geophysical Monograph, American Geophysical Union; 1974.
- Hocke K, Schlegel K. A review of atmospheric gravity waves and travelling ionospheric disturbances: 1982–1995, *Annales Geophysicae.* 1996;14:917.
- Tsagouri I, Belehaki A, Koutroumbas K, Herekakis T. Identification of large scale ionospheric travelling disturbances (Lstids) based on digisonde observations. *Atmosphere.* 2023;14:331. Available:<https://doi.org/10.3390/atmos14020331>
- Richmond A. Gravity wave generation, propagation, and dissipation in the thermosphere, *J. Geophys. Res.* 1978;83:4131.
- Hunsucker RD. Atmospheric gravity waves generated in the high latitude ionosphere: A review, *Rev. Geophys. Space Phys.* 1982;20:293.
- Jing N, Hunsucker RD. A theoretical investigation of sources of large and medium scale atmospheric gravity waves in the auroral oval, *J. Atmos. Terr. Phys.* 1993;55:1667.
- Balthazor RL, Moffett RJ. A study of atmospheric gravity waves and travelling ionospheric disturbances at equatorial latitudes. *Annales Geophysicae.* 1997;15:1048-1056.
- Ding F, Wan W, Ning B, Zhao B, Li Q, Zhang R, Xiong B, Song B. Two dimensional imaging of large scale travelling ionospheric disturbances over China based on GPS data. *J. Geophys. Res.* 2012;117:A08318.
- Ferreira AA, Borries C, Xiong C, Borges RA, Mielich J, Kouba D. Identification of potential precursors for the occurrence of large scale travelling Ionospheric disturbances in a case study during September 2017. *J. Space weather. Space Clim.* 2020;2022:10, 32.
- Fritts DC, Yuan L. Stability analysis of inertia-wave structure in the middle atmosphere. *Journal of Atmospheric Sciences.* 1989;46(12):1738-1745. Available:[https://doi.org/10.1175/1520-0469\(1989\)046<1738 : saoiws>2.0.co;2](https://doi.org/10.1175/1520-0469(1989)046<1738 : saoiws>2.0.co;2)
- Kotake N, Otsuka Y, Tsugawa T, Ogawa T, Saito A. Climatological study of GPS total electron content variations caused by medium-scale travelling ionospheric disturbances. *J. Geophys. Res.* 2006;111:1-8.
- Frissell NA, Baker JBH, Ruohoniemi JM, Greenwald RA, Gerrard AJ, Miller ES, West ML. Sources and characteristics of medium-scale travelling ionospheric disturbances observed by high frequency radars in the North America Sector. *J. Geophys. Res. Space Physics.* 2016;121: 3722-3739.
- Habarulema JB, Katamzi ZT, Yingeza E, Yamazaki Y, Seemala G. Simultaneous storm time equatorward and poleward large scale TIDs on a global scale. *Geophysical Research Letters.* 2016; 43(13):6678-6686.
- Katamzi ZT, Habarulema JB. Travelling ionospheric disturbances observed at south african mid-latitudes during the 29th – 31st October 2003 geomagnetically disturbed period. *Advances in space Research.* 2003;53(2014):48-62.
- McNamara L. The ionosphere: Communications, Surveillance and direction finding Orbit, a foundation series. Krieger Pub. Co; 1991.
- Gorelick N, Hancher M, Dixon M, Ilyushchenko S, Thau D, Moore R. Google Earth Engine: Planetary-scale geospatial analysis for everyone. *Remote Sensing and Environment.* 2017;202:18-27.
- De Graaf M, Stammes P, Torres O, Koelemeijer RBA. Absorbing aerosol index: Sensitivity analysis, application to GOME, and comparison to TOMS. *Journal of Geophysical Research: Atmospheres.* 2005;110(D1).
- Zhongming Z, Linong L, Xiaona Y, Wangqiang Z, Wei L. Satellites and Unusual Sahara dust plume; 2020.
- Asare-Ansah AB, Twumasi YA, Ning ZH, Ansah PB, Frimpong DB, Owusu F, Apraku CY, Anokye M, Loh M, Armah RDN, Opong J. Tracking The Godzilla Dust plume using the Google Earth Engine Platform. The international Archives of the photogrammetry, Remote sensing and spatial information sciences, Vol. XLVI-M-2-2022, ASPRS 2022 Annual conference, 6-8 February and 21-25 March, Denver, Colorado, USA and Virtual; 2022. Available:<https://doi.org/10.5194/isprs-Archives-XLVI-M-2-2022-33-2022>
- Althaf P, Shaeb KHB, Kumar KR. Hotspot analysis and long-term trends of Absorbing aerosol index from dust emissions were measured by the Ozone measuring Instrument at different Urban locations in India from 2005 to 2008. *Atmospheric Environment.* 2022;118933.
- Jethva H, Satheesh SK, Srinivasan J. Seasonal variability of aerosols over the Indo-Gangetic basin. *Journal of Geophysical Research: Atmospheres.* 2005;110(D21).
- Gorelick N, Hancher M, Dixon M, Ilyushchenko S, Thau D, Moore R. GoogleEarth Engine: Planetary-scale geospatial analysis for everyone. *Remote sensing and Environment.* 2017;202:18-27.
- Gurtner W, Estey L. Rinex-the receiver independent exchange format-

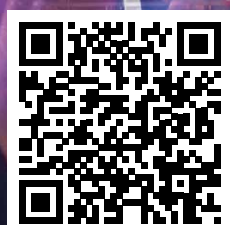
- version3.00. Astronomical Institute, University of Bern and UNAVCO, Boulder, Colorado;2007.
25. Seemala GK. GPS-TEC Analysis Application Read Me. Institute for Scientific Research, Boston College, USA; 2011.
 26. Tariku YA. Patterns of GPS-TEC variation over low-latitude regions (African sector) during the deep solar minimum (2008 to 2009) and solar maximum (2012 to 2013) phases. *Earth, Planets and Space*. 2015;67(1):1–9.
 27. Horvath I, Crozier S. Software developed for obtaining GPS-derived total electron content values. *Radio Science*. 2007; 42(02):1–20.
 28. Cepni MS, Potts LV, Miima JB. High-resolution station- based diurnal ionospheric total electron content (TEC) from dual-frequency GPS observation *Space Weather*. 2013;11(9): 520–528.
 29. Ma X, Maruyama T, Ma G, et al. Three-dimensional ionospheric tomography using observation data of gps ground receivers and ionosonde by neural network. *Journal of Geophysical Research: Space Physics*. 2005;110(A5).
 30. Jin S, Park J, Wang J, Choi B, Park P. Electron density profiles derived from ground-based observations. *The Journal of Navigation*. 2006;59(3):395-401.
 31. Heise S, Jakowski N, Wehrenpfennig A, et al. Sounding of the topside ionosphere/plasmasphere based on GPS measurements from champ: Initial results. *Geophysical Research Letters*. 2002; 29(14):44–1.
 32. Jawoski N, Mayer C, Hoque M, Wilken V. Total electron content models and their use in ionosphere monitoring. *Radio Science*. 2011;46(06):1-11.
 33. Ciraolo L, Azpilicueta F, Brunini C, Meza A, Radicella SM. Calibration errors on experimental slant total electron content determined by the GPS. *Journal of Geodesy*. 2007;81:111-120.
 34. Kassa T, Damtie B. Ionospheric irregularities over Bahir Dar, Ethiopia during selected geomagnetic storms, *Advances in Space Research*; 2017 Available:<http://dx.doi.org/10.1016/j.asr.2017.03.036>
 35. Otsuka Y, Ogawa T, Saito A, Tsugawa T, Fukao S, Miyazaki S. A new technique for mapping of total electron content using GPS network in Japan. *Earth, Planets and Space*. 2002;54(1):63-70.
 36. Sardon E, Zarraoa N. Estimation of total electron using GPS data: How stable are the differential satellite and receiver instrumental biases? *Radio Science*. 1997;32(5):1899-1910.
 37. Aryal S, Geddes G, Finn S, et al. Multi-spectral and Multi-instrumentation Observation of TIDs following the solar eclipse of 21st August 2017. *Journal of Geophysical Research: Space Physics*. 2019;124.
 38. Zhang SR, Coaster AJ, Erickson PJ, Goncharenko LP, Rideout W, Vierinen J. Travelling ionospheric disturbances and ionospheric perturbations associated with solar flares in September 2017. *Journal of Geographical Research: Space Physics*. 2019;124(7):5894-5917.
 39. Zakharenkova I, Astafyeava E, Cherniak I. GPS and GLONAS observations of large-scale travelling ionospheric disturbances during the 2015 St. Patrick's day storm. *Journal of Geophysical Research: Space Physics*. 2016;121(12):12-138. Available:<https://doi.org/10.1002/2016ja032332>
 40. Warren C. Godzilla dust storm traced to shaky northern jet stream; 2023. Available:<https://www.science.org/content/article/godzilla-dust-storm-Traced-shaky-northern-jet-stream>, 2022
 41. Kamide Y, Chian A. *Hand Book of the Solar-Terrestrial environment*. Springer Berlin Heidelberg, New York. ISBN 978-3-540-46314-6; 2007 DOI: 10.007/6104478
 42. VanZandt TE. A universal spectrum of buoyancy waves in the atmosphere. *Geophys. Res. Lett*. 1982;9:575- 578.
 43. Balsley BB, Carter DA. The spectrum of atmospheric velocity fluctuations at 8 and 86 km. *Geophys. Res. Lett*. 1982;9:465–468.
 44. Nakamura T, Tsuda T, Fukao S, Kato S, Manson AH, Meek CE. Comparative observations of short-period gravity waves (10-100 min) in the mesosphere in 1989 by Saskatoon MF radar (52on), Canada and the MU radar (35on), Japan. *Radio Sci*. 1993;28:729–746.
 45. Collins RL, Nomura A, Gardner CS. Gravity waves in the upper mesosphere over Antarctica: Lidar observations at the South Pole and Syowa. *J. Geophys. Res*. 1994;99:5475–5485.
 46. Jonah OF, Zhang S, Coster AJ, Goncharenko LP, Erickson PJ, Rideout W, De Paula ER, De Jesus R. Understanding Inter-Hemispheric Traveling Ionospheric Disturbances and Their Mechanisms. *Remote Sens*. 2020;12:228.
 47. Dhadly M, Sassi F, Emmert J, Drob D, Conde M, Wu Q, Makela J, Budzien S, Nicholas A. Neutral winds from mesosphere to thermosphere—past, present, and future outlook. *Front. Astron. Space Sci*. 9: 1050586. DOI: 10.3389/fspas.2022.1050586
- The paper originally published in International Astronomy and Astrophysics Research Journal may be cited as: Edward, Uluma, Chali Idosa Uga, Solomon Otoo Lomotey, Athwart Davis Odhiambo, Fashae Joshua Bankole, Kouassi Nguessan, Muniafu Wilberforce, Boniface Ndinya, and Omondi George. 2024. "Observation of Travelling Ionospheric Disturbances over Morocco During the Godzilla Sand and Dust Storm of 15th to 26th June 2020 Using GNSS". International Astronomy and Astrophysics Research Journal 6 (1): 18-39. <https://www.journaliaarj.com/index.php/IAARJ/article/view/100>.*
- © Copyright (2024): Author(s). The licensee is the journal publisher. This is an Open Access article distributed under the terms of the Creative Commons Attribution License (<http://creativecommons.org/licenses/by/4.0>), which permits unrestricted use, distribution, and reproduction in any medium, provided the original work is properly cited. The article is republished with author's permission. ▽

INTERGEO[®] 2024

SEPT. 24 – 26
STUTT GART

**INSPIRATION
FOR A SMARTER
WORLD**

WWW.INTERGEO.DE



GET YOUR

TICKET NOW!

VOUCHER CODE: IG24-MC

EXPO CONFERENCE STAGE NETWORKING



Host: DVW e.V.
Conference organiser: DVW GmbH
Expo organiser: HINTE Expo & Conference GmbH

SPONSORS:



GNSS Constellation Specific Monthly Analysis Summary: July 2024

The analysis performed in this report is solely his work and own opinion. State Program: U.S.A (G); EU (E); China (C) "Only MEO- SECM satellites"; Russia (R); Japan (J); India (I)



Narayan Dhital

Actively involved to support international collaboration in GNSS-related activities. He has regularly supported and contributed to different workshops of the International Committee on GNSS (ICG), and the United Nations Office for Outer Space Affairs (UNOOSA). As a professional employee, the author is working as GNSS expert at the Galileo Control Center, DLR GfR mbH, Germany.

Introduction

The article is a continuation of monthly performance analysis of the GNSS constellation. In this month’s issue, there is an additional discussion on the periodicity of the satellite atomic clock offset.

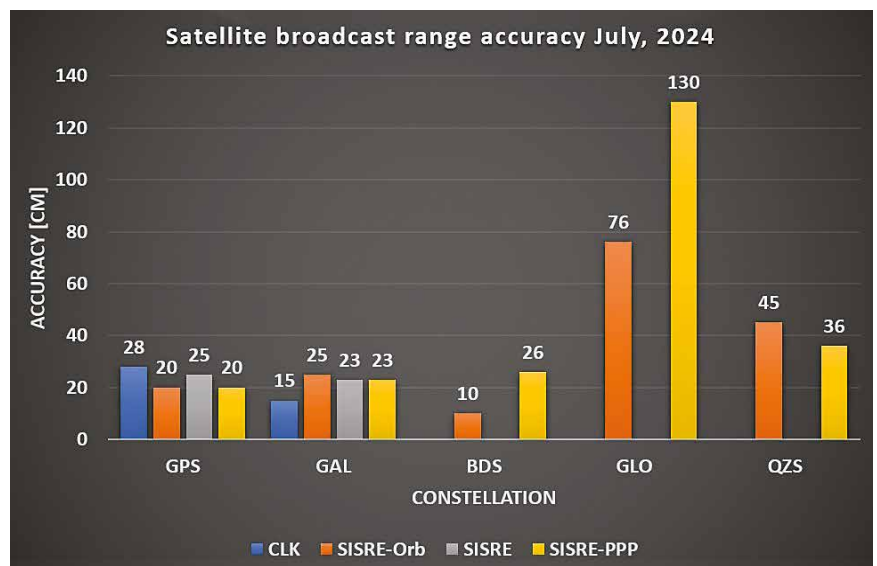
Analyzed Parameters for July, 2024

(Dhital et. al, 2024) provides a brief overview of the necessity and applicability of monitoring the satellite clock and orbit parameters

- a. Satellite Broadcast Accuracy, measured in terms of **Signal-In-Space Range Error (SISRE)** (Montenbruck et. al, 2010).

- b. **SISRE-Orbit** (only orbit impact on the range error), **SISRE** (both orbit and clock impact), and **SISRE-PPP** (as seen by the users of carrier phase signals, where the ambiguities absorb the unmodelled biases related to satellite clock and orbit estimations. Satellite specific clock bias is removed) (Hauschlid et.al, 2020)
- c. **Clock Discontinuity**: The jump in the satellite clock offset between two consecutive batches of data uploads from the ground mission segment. It is indicative of the quality of the satellite atomic clock and associated clock model.
- d. **URA**: User Range Accuracy as an indicator

(a), (b) Satellite Clock and Orbit Accuracy (monthly RMS values)



of the confidence on the accuracy of satellite ephemeris. It is mostly used in the integrity computation of RAIM.

- e. **GNSS-UTC offset:** It shows stability of the timekeeping of each constellation w.r.t the UTC
- f. **Satellite Clock Offset Fourier Analysis:** The knowledge of a periodic behavior of the on-board atomic clock offset is essential for better prediction model.

Note:- for India’s IRNSS there are no precise satellite clocks and orbits as they broadcast only 1 frequency which does not allow the dual frequency combination required in precise clock and orbit estimation; as such, only URA and Clock Discontinuity is analyzed.

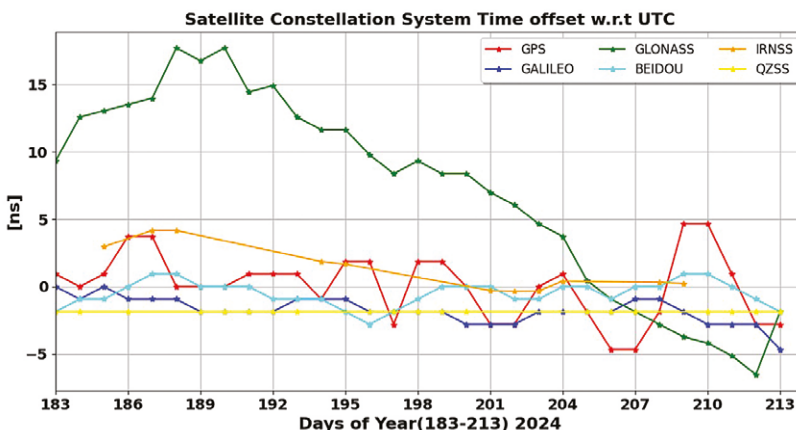
(c) Satellite Clock Jump per Mission Segment Upload

Const	Mean [ns]	Max [ns]	95_Percentile [ns]	99_Percentile [ns]	Remark (Best and Worst 95 %)
IRNSS	7.78	4017.66	6.26	26.87	Best I02 (4.21 ns) Worst I06 (14.77 ns) I03 is not there in BRDC
GPS	0.41	6.56	0.94	2.11	Best G04 (0.33 ns) Worst G21 (2.14 ns) No such large jumps as in previous months
GAL	6.10	461428.8	0.18	0.43	Best E31 (0.14 ns) Worst E12 (0.21 ns) Large jump for E04 on DOY 189, large jump ofr E12 on DOY 203

(d) User Range Accuracy (Number of Occurrences in Broadcast Data 01–31 July)

IRNSS-SAT	2 [m]	2.8 [m]	4.0 [m]	5.7 [m]	8 [m]	8192 [m]	9999.9 [m]	Remark Other URA values (frequency)
I02	2971	26	2	-	1	7	-	11.3 (1)
I03	-	-	-	-	-	-	-	-
I06	718	2	2	-	5	-	1	32 (1) 11.3 (1)
I09	573	5	2	1	1	-	-	-
I10	471	3	1	-	-	-	-	-

(e) GNSS-UTC Offset



(f) Satellite Clock Offset Fourier Analysis

The atomic clocks on-board satellites are influenced by various phenomena such as the J2 term, Earth oblateness, satellite thermal radiation, and estimation errors induced by satellite orbits. These periodic variations in the satellite clock data are often absorbed by the satellite clock offset, resulting in periodic signals if not properly modeled. A quadratic polynomial fit (QPM) of the reference satellite clock offset serves as a starting point for analysis. The residuals of the QPM for different satellites and atomic clock types reveal variations due to differing orbits.

A simple Fast Fourier Transform (FFT) analysis highlights these periodic components. For Medium Earth Orbit (MEO) satellites like GPS, GAL, and BDS, the twice-per-day term is prominent, reflecting their MEO orbit period. In contrast, Geostationary Earth Orbit (GEO) and Inclined Geosynchronous Orbit (IGSO) satellites (C04 and C10, respectively) exhibit different periodic terms. For GEO satellites, the dominant term is the 1 cycle per day, with its harmonics decreasing in strength with integer multiples.

The plots in Figure f(a) and f(b), visually represents these periodicities. The time series of the residuals (f(a)) obtained by subtracting the satellite clock offset from the QPM predicted values show distinct oscillations for Beidou IGSO and GEO on-board atomic clock. For atomic clocks on-board the MEO orbit the residuals are not stark. However, G08 shows a lot of noise and variation in the residuals and this is due to the Cesium frequency standard used in G08, for which linear model is more suitable than the QPM. The significant peaks at specific frequencies (in f(b)) indicate the presence of pronounced periodic components in the satellite clock offsets. These peaks correspond to the periodic terms discussed, with MEO satellites showing strong twice-per-day components and GEO satellites displaying daily cycles and their harmonics.

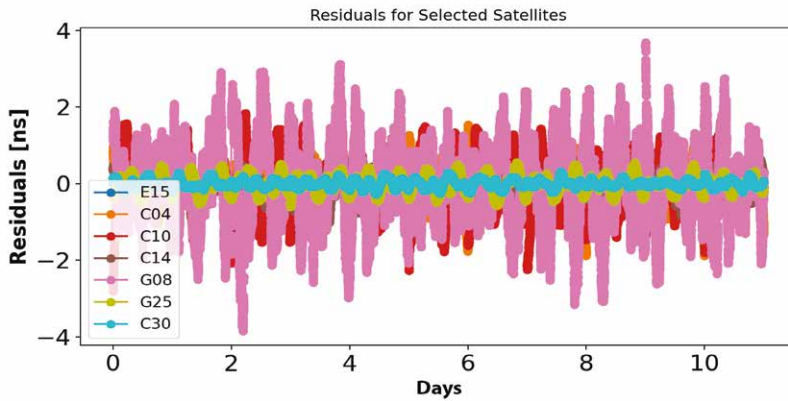


Figure f (a): The QPM fitting of the satellite clock offset is shown as the time series for sample 11 days from the past (09–20 Jan, 2021). Depending on the type of atomic clocks and satellite orbits, the residuals have different oscillating pattern and amplitudes.

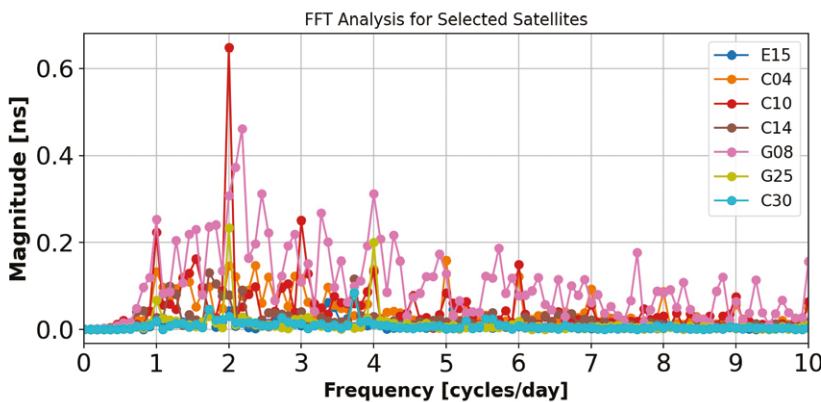


Figure f (b): The FFT of the QPM residuals for different satellite atomic clocks flying on various satellite orbits. As the time period of the analysis is only 11 days (Jan 9–20, 2021, GFZ Final Clocks), the primary components might not be reflected properly. The longer the time period for FFT analysis, the better the resolution and detection of correct components. The FFT in this context is mostly to serve the residuals analysis in f(a).

The temporal variation of amplitudes and the prime frequency components for satellites are crucial for understanding the stability and accuracy of satellite clocks. Temporal variations can indicate changes in the satellite’s environment or operational conditions, which can affect the clock’s performance. By analyzing these variations, constellation service provider can identify and mitigate potential sources of error.

Short-Time Fourier Transform (STFT) can be used to analyze these temporal variations by providing a time-frequency representation of the signal. STFT allows for the observation of how the frequency components of the satellite clock offsets change over time, offering a more detailed understanding of the periodic effects. This analysis helps to better solidify the clock

model by identifying transient behaviors and ensuring that the model accurately reflects the satellite’s performance over its operational period. In general, the GNSS satellite atomic clocks demonstrate the temporal variation in amplitude and frequency. The assessment of such variations and in-dept periodicity analysis of different satellite atomic clocks will be provided in the future issue of the article.

Monthly Performance Remarks:

1. Satellite Clock and Orbit Accuracy:
 - For GPS, the satellite clock and orbit accuracy shows slight performance improvement.
 - For Galileo, all parameters showed consistent performances. Satellite E12 has a large clock jump on DOY 203 around 18:00 UTC. There was a missing BRDC data for 1 hour and

right afterwards the satellite was set to NAPA. Further check is needed as it could be a near fault event.

- For GLONASS, the performance looked similar to the past months.
- For BDS and QZSS, the performance looks very much the same as in the past.
- For IRNSS, the notable difference in this month’s performance is the URA for I03. There is no broadcast record. For I02 and I06, a new URA value of 11.3 was recorded.

2. UTC Prediction (GNSS-UTC):

- High oscillation of GPS-UTC between DOY 208–2013. GLONASS had large offset that started to decrease after DOY 189 and reached finally within 5 ns level.

References

- Alonso M, Sanz J, Juan J, Garcia, A, Casado G (2020) Galileo Broadcast Ephemeris and Clock Errors Analysis: 1 January 2017 to 31 July 2020, MDPI
- Alonso M (2022) Galileo Broadcast Ephemeris and Clock Errors, and Observed Fault Probabilities for ARAIM, Ph.D Thesis, UPC
- Cao X, Zhang S, Kuang K, Liu T (2018) The impact of eclipsing GNSS satellites on the precise point positioning, *Remote Sensing* 10(1):94
- Dhital N (2024) GNSS constellation specific monthly analysis summary, *Coordinates*, Vol XX, Issue 1, 2, 3, 4
- Hauschlid A, Montenbruck O (2020) Precise real-time navigation of LEO satellites using GNSS broadcast ephemerides, *ION*
- Guo F, Zhang X, Wang J (2015) Timing group delay and differential code bias corrections for BeiDou positioning, *J Geod*,
- IERS C04 (2024) <https://hpiers.obspm.fr/iers/eop/eopc04/eopc04.1962-now>

ISRO launches Earth Observation Satellite EOS-08

Indian Space Research Organisation's latest Earth Observation Satellite 'EOS-08' was launched by the Small Satellite Launch Vehicle (SSLV)-D3 on August 16, 2024 at 9:17 hrs from Satish Dhawan Space Centre, Sriharikota.

The primary objectives of the EOS-08 mission include designing and developing a microsatellite, creating payload instruments compatible with the microsatellite bus, and incorporating new technologies required for future operational satellites.

Built on the Microsat/IMS-1 bus, EOS-08 carries three payloads: Electro Optical Infrared Payload (EOIR), Global Navigation Satellite System-Reflectometry payload (GNSS-R), and SiC UV Dosimeter. The EOIR payload is designed to capture images in the Mid-Wave IR (MIR) and Long-Wave IR (LWIR) bands, both during the day and night, for applications such as satellite-based surveillance, disaster monitoring, environmental monitoring, fire detection, volcanic activity observation, and industrial and power plant disaster monitoring.

The GNSS-R payload demonstrates the capability of using GNSS-R-based remote sensing for applications such as ocean surface wind analysis, soil moisture assessment, cryosphere studies over the Himalayan region, flood detection, and inland waterbody detection. Meanwhile, the SiC UV Dosimeter monitors UV irradiance at the viewport of the Crew Module in the Gaganyaan Mission and serves as a high-dose alarm sensor for gamma radiation.

EOS-08 marks a significant advancement in satellite mainframe systems such as an Integrated Avionics system, known as the Communication, Baseband, Storage, and Positioning (CBSP) Package, which combines multiple functions into a single, efficient unit. This system is designed with cold redundant systems using commercial off-the-shelf (COTS) components and evaluation boards, supporting up to 400 Gb of data storage. Additionally, the satellite includes a structural panel embedded with PCB, an embedded battery, a Micro-DGA (Dual Gimbal Antenna), an M-PAA (Phased Array Antenna), and a flexible solar panel, each serving as key components for onboard technology demonstration.

The satellite employs a miniaturized design in its Antenna Pointing Mechanisms, capable of achieving a rotational speed of 6 degrees per second and maintaining a pointing accuracy of ± 1 degree. The miniaturized phased array antenna further enhances communication capabilities, while the flexible solar panel incorporates a foldable solar panel substrate, GFRP tube, and CFRP honeycomb rigid end panel, offering improved power generation and structural integrity. A pyrolytic graphite sheet diffuser plate, known for its high thermal conductivity of 350 W/mK, reduces mass and finds application in various satellite functions. Furthermore, the EOS-08 mission adopts a new method of integrating housekeeping panels using a hinge-based fixture, significantly reducing the duration of the Assembly, Integration, and Testing (AIT) phase.

Incorporating additional novel schemes, the EOS-08 mission improves satellite technology through X-band data transmission, utilizing pulse shaping and Frequency Compensated Modulation (FCM) for X-Band data transmitters. The satellite's battery management system employs SSTCR-based charging and bus regulation, sequentially including or excluding strings at a frequency of 6 Hz.

The mission's indigenization effort is evident in its solar cell fabrication processes and the use of a Nano-Star Sensor for Microsat Applications. Additionally, the inertial system benefits from reaction wheel isolators that attenuate vibrations and a single antenna interface is utilized for TTC and SPS applications. Thermal management is enhanced using materials such as AFE BGA, Kintex FPGA, Germanium Black Kapton, and STAMET (Si-Al Alloy) Black Kapton to handle the thermal properties of COTS components. The mission also incorporates an auto-launch pad initialization feature, further demonstrating its commitment to innovative mission management. www.pib.gov.in

IGS (2021) RINEX Version 4.00 https://files.igs.org/pub/data/format/rinex_4.00.pdf

Li M, Wang Y, Li W (2023) performance evaluation of real-time orbit determination for LUTAN-01B satellite using broadcast earth orientation parameters and multi-GNSS combination, GPS Solutions, Vol 28, article number 52

Li W, Chen G (2023) Evaluation of GPS and BDS-3 broadcast earth rotation parameters: a contribution to the ephemeris rotation error Montenbruck O, Steigenberger P, Hauschlid A (2014) Broadcast versus precise ephemerides: a multi-GNSS perspective, GPS Solutions

Liu T, Chen H, Jiang Weiping (2022) Assessing the exchanging satellite attitude quaternions from CNES/CLS and their application in the deep eclipse season, GPS Solutions 26(1)

Montenbruck O, Steigenberger P, Hauschlid A (2014) Broadcast versus precise ephemerides: a multi-GNSS perspective, GPS Solutions

Montenbruck O, Hauschlid A (2014 a) Differential Code Bias Estimation using Multi-GNSS Observations and Global Ionosphere Maps, ION

Steigenberger P, Montenbruck O, Bradke M, Ramatschi M (2022) Evaluation of earth rotation parameters from modernized GNSS navigation messages, GPS Solutions 26(2)

Sylvain L, Banville S, Geng J, Strasser S (2021) Exchanging satellite attitude quaternions for improved GNSS data processing consistency, Vol 68, Issue 6, pages 2441-2452


Walter T, Blanch J, Gunning K (2019) Standards for ARAIM ISM Data Analysis, ION

Wang N, Li Z, Montenbruck O, Tang C (2019) Quality assessment of GPS, Galileo and BeiDou-2/3 satellite broadcast group delays, Advances in Space Research

Note: References in this list might also include references provided to previous issues.

Data sources:

<https://cdis.nasa.gov> (Daily BRDC); http://ftp.aiub.unibe.ch/CODE_MGEX/CODE/ (Precise Products); BKG "SSRC00BKG" stream; IERS C04 ERP files

(The monitoring is based on following signals- GPS: LNAV, GAL: FNAV, BDS: CNAV-1, QZSS:LNAV IRNSS:LNAV GLO:LNAV (FDMA)) 

Digital Twins – A panacea for development?

Digital twins will undoubtedly become a critical requirement for organizations and countries in the future.



Dr Siva Kumar Rachapudi
Managing Director
SIBHU
siva@sibhu.space

There has been increased interest in Digital Twins (DT) in India, and the growth of startups in this domain is mushrooming. It is pertinent to understand the evolution of these technologies, which requires a comprehensive understanding of various underlying complexities and the basic requirement of ground truthing. In the past, many organizations, both public and private, have ventured into new areas without realizing the need for in-depth knowledge of interdisciplinary subjects, including geospatial technologies. It is envisaged that the ‘Sangam: Digital Twin’ initiative will propel India towards becoming a developed country by 2047. To realize this vision, we need to raise awareness and create conditions that enable startups to achieve unicorn status.

What is Digital Twin

A digital twin is a virtual representation of a physical object, process, or system that serves as a real-time digital counterpart. It acts as a digital replica of a real-world entity or system, used for simulation, analysis, monitoring, and prediction. The physical entity and its digital model are connected through real-time data. Digital twins are increasingly applied in various fields, including smart cities, healthcare, aerospace, manufacturing, and oil & gas, to support informed decision-making, maintenance, risk reduction, and performance enhancement.

Geospatial technologies, combined with the Internet of Things (IoT), Artificial Intelligence (AI), Machine Learning (ML), and Big Data analytics, form the core of digital twins. These technologies enable organizations to better understand, predict,

and optimize the performance of their assets or processes. The full potential of digital twins is still being explored.

Digital Twins in India

The adoption of digital twin technology in India is growing, driven by government initiatives and private sector innovation. Many projects across various sectors are being implemented, for Smart Cities as part of the Smart Cities Mission (Pune, Bangaluru, Varanasi), manufacturing (TCS), infrastructure (L&T), healthcare (facilities managements), energy sector (power plants for performance optimization), agriculture (precision agriculture, crop management), education (virtual labs, training), transportation (traffic management and urban planning), utilities management (sewage. Waste disposal, distribution of power, gas), digital heritage (Hampi, Nalanda).

Digital Twin and 3D GIS

While 3D GIS (Geographic Information System) and digital twins are related technologies, they are not the same. 3D GIS focuses on spatial data representation and analysis with geographic and topographic information typically static or updated periodically for visualization and spatial analysis. By integrating IoT, it becomes a real-time dynamic system.

Whereas Digital Twin represents a specific object, system, or process, incorporates various types of data beyond just geographic information including real-time data enabling simulation and

predictive analysis. It can effectively be used for monitoring, optimization, prediction, preventive maintenance and informed decision-making

However, 3D GIS can be a component of a digital twin, especially for location-based digital twins as digital twins often incorporate GIS data and functionality. - A digital twin may use 3D GIS as its base layer, adding real-time data and simulation capabilities

In essence, while 3D GIS provides a spatial foundation, a digital twin goes beyond by incorporating real-time data, simulation capabilities, and a broader range of information types. A digital twin can be more dynamic and interactive than a traditional 3D GIS model.

First 3D GIS Project – Chandni Chowk Delhi

Traditionally, GIS was used for mapping and decision-making in 2D throughout the last century. However, with advances in computing and communication technologies, the concept of 3D GIS began to be implemented in various developed nations at the turn of the century. In 2006, the Department of Science & Technology conducted a pilot project in Chandni Chowk, one of Delhi's oldest and busiest markets. This project aimed to create a detailed 3D model of Chandni Chowk for urban planning, heritage conservation, law enforcement, and infrastructure management.

Contemporary technologies such as high-resolution aerial photography, satellite imagery, LiDAR (Light Detection and Ranging), and GPR (Ground Penetrating

Radar), complemented by ground surveys, were used for data collection.

There were many challenges in the form of complexity of the area with narrow lanes and dense construction, integration of modern technology with historical architecture, incorporation of cadastral data, temporal accuracy of data in a rapidly changing urban environment.

Delhi 3D GIS – Delhi Geospatial Act 2011

Encouraged by the success of this project, the Delhi Government undertook the creation of a 3D GIS for the entire city, covering 1,500 square kilometers, starting in 2008. This project marked the first comprehensive 3D GIS in the country, efficiently planned and executed by the Survey of India (SOI) with private sector participation. SOI employed innovative methods and processes for data collection, productization, and tools, offering diverse applications and services through the Delhi Geoportal. Additionally, SOI successfully transferred knowledge to Delhi officials at various levels, which contributed to the enactment of India's first geospatial legislation, the Delhi Geospatial Act of 2011.

Today, Geospatial Delhi Limited (GSDL), a Geo-Knowledge enterprise and custodian of Spatial Data Infrastructure (SDI), maintains and updates spatial data through mapping and surveys. GSDL facilitates the usage of this data across various departments in Delhi. As a unique Spatial Data Resource Center, GSDL integrates data from various departments, standardizing and ensuring interoperability. By

generating relationships that reflect real-world scenarios, GSDL serves the data through value-added applications. It provides a flexible set of GIS tools, geospatial services, and applications to support the diverse functions handled by the Delhi Government.

First Digital Twin Project – Indian Digital Heritage Project – Digital Hampi

The Digital Hampi Project is an innovative initiative aimed to digitally preserve and showcase the UNESCO World Heritage Site of Hampi, located in Karnataka, India. Leveraging the experience gained from 3D GIS technology, the project goes beyond future planning to revive and reconstruct the past. It involves recreating destroyed monuments, building 3D models, and tagging various aspects of social life, culture, art, dance, and music to provide an immersive experience for users.

The project utilizes 3D laser scanning, terrestrial photogrammetry, and Virtual and Augmented Reality (VR/AR) to create high-resolution 3D models of monuments and artifacts.

In 2011, the Department of Science and Technology (DST) convened researchers from 24 premier research and academic institutes across India to focus on the digital documentation and interpretation of tangible and intangible heritage. The initiative aimed to extend the capabilities of digital technologies beyond mere monuments to encompass art, architecture, and all forms of cultural and historical knowledge.

By leveraging advanced technologies in computer vision, graphics, augmented and immersive experiences, as well as audio-video technologies and user interface design, the project sought to create vivid representations of heritage. These technologies provide users with immersive experiences and offer analytic tools for art historians, architects, and scholars interested in conducting in-depth studies of Indian heritage.

3D GIS provides a spatial foundation, a digital twin goes beyond by incorporating real-time data, simulation capabilities, and a broader range of information types. A digital twin can be more dynamic and interactive than a traditional 3D GIS model.

While there are many commercial applications that can utilize digital twin technology, there can be many areas for military application. Digital twins enable defence organizations to monitor the health and performance of military assets in real-time.

The basic goal of the IDH project was to bring about a fine synergy of Geospatial technologies with matured ICT technologies and develop technology tools to help preserve, use, and experience India's vast heritage in digital form. Such a task could only be achieved by collaboration among different communities and agencies : the technology community consisting of scientists and engineers from, who would invent, innovate and develop appropriate technologies, the culture community consisting of 11 teams of artists, art historians, archaeologists, architects, anthropologists and other experts from the humanities and the social sciences who know and understand the heritage, government agencies who as custodians of India's vast heritage bring the necessary executive power to enable the collaboration, and private agencies, companies and other organization interested in this for a variety of reasons including tourism. This was perhaps the first such effort in India attempted as a major multi-disciplinary, multi-institutional, multi-crore project supported by the Department of Science and Technology through its arm Natural Resources Data Management Systems (NRDMS).

Digital Twins for national security

While there are many commercial applications that can utilize digital twin technology, there can be many areas for military application. Digital twins enable defence organizations to monitor the health and performance of military assets in real-time. By collecting and analyzing data from sensors embedded in the

physical systems, digital twins can detect anomalies, predict failures, and optimize maintenance schedules. This proactive approach to maintenance minimizes downtime, reduces costs, and enhances the readiness of military equipment.

Training on equipment, weapons, delivery systems and surveillance systems:

Digital twin can enable display of the equipment structure, machine status, and mechanical principles, for effective transfer of knowledge to personnel with varying capabilities. Thus, it can effectively increase the learning experience of students while decreasing the cost (both time and money) of trying to use an actual machine. It integrates real-scene 3D modelling technology, big data technology, etc. to build a digital twin platform for military training scenes, which can realize the organic combination of people, equipment, and environment virtual and reality, and form a dynamic virtual presentation of the battlefield environment. In future it should be possible to accurately simulate in real time all five senses allowing soldiers to feel the flames of war.

Decision Making:

Scenario generation, mission planning and decision-making processes greatly improved by integrating real-time data from multiple sources, including sensors, intelligence systems, and geographical information providing commanders with a comprehensive situational awareness. Digital twin allows for an accurate and real time assessment of the battlefield and gives commanders the ability to make the best possible decisions to lead to victory.

Logistics and Maintenance:

Full life cycle management will allow for effective anticipation of repair needs creates a record of data used in digital twins to accurately predict when equipment will need repairs and even help predict potential maintenance issues if the product is changed or upgraded.

Military readiness requires resilient, battlefield ready supply chains across the defence enterprise. Digital twins are a critical tool in this environment and can help manage supply chain risk, accelerate reinvention and build resiliency by combining human ingenuity with technologies that fuel end-to-end visibility and AI-powered scenario modelling. Predictive analytics tools would help. Battlefield logistics needs, and solve problems such as battlefield equipment failures and logistics with high quality and efficiency by efficient supply chain management.

Challenges

A number of challenges many organizations face such as complex data management, skills (AI & ML) and knowledge upgradation of staff, efficient cyber security protocols and their strict adherence, higher costs of recovery platforms for data and solutions, dependence on a number of vendors/suppliers. More important lack of awareness even at leadership levels.

Another issue is the quality, volume and complexity of data needed and the time and costs involved in managing it.

The turf war across agencies within and outside the organizations creates duplication resulting in higher expenses and lack of standardization leads to interoperability issues. Data sharing amongst stakeholders is still an issue besides Ownership of Physical and Digital Models, Intellectual Property Rights (IPR), Data Integrity and Security. Standardized contract templates be used for Systems integrators drawing data,

solutions and services from multiple agencies to ensure effective and efficient maintenance and to keep them current in real time/near real time.

Conclusion

Digital twins will undoubtedly become a critical requirement for organizations and countries in the future. To use these technologies effectively and optimize resources, developing nations will need comprehensive legislation to prevent misuse and protect safety, privacy, and national security.

While many startups are emerging in this field, there is a need for mentorship and support to help these startups grow into successful unicorns. To facilitate this, exclusive programs focused on digital twins should be organized to increase awareness, outreach, and provide necessary training and mentoring. Establishing nationwide Centers of Excellence can play a crucial role in this effort.

Developing human resources for digital twin implementation in defence forces is crucial. Military officers made significant contributions in geospatial as a part of Survey of India. Now that the military survey is becoming a self-sufficient agency, there is a crying need to establish a Capability Centre for Specialized training programs, Cross-disciplinary education, Partnerships with academia and industry and change management.

We also have to debate the need for an exclusive Geospatial Act for the country encompassing all geospatial and related technologies. Government may provide more incentives for startups to enable them to compete for the projects and provide support for research and innovation by startups in various sectors such as Automobile, Infrastructure, Revenue, Agriculture, Defence & Homeland security, traffic management on land, air and sea, public places and heritage buildings, etc. ▽

Chile space cooperation agreement with Brazil

Chile and Brazil signed a Memorandum of Understanding on Cooperation in Space Activities for Peaceful Purposes, to promote joint programs and projects in space matters. Both countries will identify areas to develop joint programs and projects by their respective national policies on space policy. www.gob.cl

Neuraspace partnership with EISCAT on Space Traffic Management

This strategic partnership gives Neuraspace access to radar observation time for monitoring space objects. It will also provide advanced ionospheric and atmospheric measurement data, in preparation for using the next generation of the incoherent scatter radar facility EISCAT_3D.

EISCAT Scientific Association has been providing access to high-latitude incoherent radar scattering facilities and other instrumentation for scientific, non-military purposes since 1980.

Partnering with EISCAT also allows Neuraspace to collaborate with the wider community of experts, fostering innovation in STEM research and development. neuraspace.com

Apex releases GEO Satellite Bus

Apex announced the introduction of GEO Aries, a productized ESPA-class satellite bus designed for geostationary orbit (GEO) missions. It is a high delta-v satellite bus designed to support the needs of Apex's customers' GEO missions, including communications, imaging, and other use cases. www.apexspace.com

Lockheed Martin to acquire Terran Orbital

Lockheed Martin shall acquire Terran Orbital, a global leader of satellite-based solutions primarily supporting the aerospace and defense industries.

Terran Orbital brings a high throughput, robotic manufacturing capacity and high-performing modular space vehicle designs. Lockheed Martin uses It's satellites for its work, most notably with the Space Development Agency's Transport and Tracking Layer programs, and in several of its self-funded technology demonstrations. lockheedmartin.com

World's first satellite exclusively for observing biodiversity

Kongsberg NanoAvionics has announced that four of their customer satellites, will be launched into orbit aboard the upcoming SpaceX Transporter-11 mission. All these nanosatellites built by NanoAvionics, include the world's first satellite dedicated exclusively to observing the Earth's biodiversity (which will also become Chile's first private satellite), a mission to monitor the health of our oceans, using a hyperspectral imager for Earth observation, and a communication mission with a software-defined radio (SDR) payload.

The 6U "Lemu Nge" (Forest Eye) will use an onboard hyperspectral camera to capture high-resolution images of 4.75m GSD (ground sampling distance) of the world's forests in over 30 visible and infrared bands. With the data Chilean company Lemu is building an atlas of the Earth's biosphere that can be used to develop and evaluate conservation plans and sustainability strategies. nanoavionics.com

Satellite Data + AI help manage smart cities

SkySat data has been leveraged by the government of the Kingdom of Bahrain's Survey and Land Registration Bureau (SLRB), to enhance urban planning initiatives nationwide. In collaboration with Planet, Aetosky has implemented an advanced urban planning system. This turnkey solution integrates AI-enabled change detection technology with high-resolution satellite imagery, exemplifying a sophisticated approach to modern urban management. www.planet.com ▽

Innovative solution for relief printing without limiting heights

Since 2014, IGN has been monitoring advancements in technology to explore a colour relief printing service for on-demand mapping



François Lecordix
National Institute of
Geographic and Forest
Information, France

Abstract

By following advancements in 3D printing technology, IGN explored an inkjet-based relief printing solution proposed by the Océ company in 2015. The initial results were presented at the International Cartographic Conference in Rio de Janeiro, showcasing the Belle-Ile map. This technology addressed several critical needs for relief mapping, including high printing resolution, large size, and accurate colour reproduction. However, it still faced two significant issues: high production costs for the general public (compared to thermoformed maps produced in multiple copies) and limited printing heights (less than 2-3 cm). In 2022, IGN introduced an innovative solution to address the limitation of printing heights without increasing production costs. This new approach combines the previous inkjet relief printing technology with Stratoconception® technology from the 3D printing domain. The details of this solution, along with an example result, are presented in this paper.

1. Introduction

During the Second World War, the demand for relief maps surged on both sides of the conflict, leading to the development of new production methods. For example, the American ribbon method (Sutter et al., 2006) accelerated the creation of initial moulds, while the German Wenschow method (Reed, 1946) also contributed to faster production. After the war, the Americans, inspired by Wenschow's approach, adopted thermoplastic sheeting to develop the thermoforming process,

which still remains the solution for producing relief maps worldwide.

In France, for instance, the National Institute of Geographic and Forest Information (IGN France) continues to produce relief maps using the thermoforming process. They print on vinyl sheets and use specially created moulds, provided that the mapped area generates enough demand to justify the costs of producing the various intermediate models. The minimum threshold for producing a first edition of relief maps is approximately one thousand copies.

However, there is a growing need for on-demand relief mapping across the country. This demand is also evident on a global level, as demonstrated by the TouchTerrain web service, which recorded 38 requests per day for print-ready digital terrain models between July 2019 and January 2021 (Harding, 2021). Despite this, the 3D prints produced by TouchTerrain are monochrome. Users must either hand-colour their 3D prints or supplement them with 2D colour maps to effectively combine the relief and paper mapping.

While there is a clear need for on-demand 3D printing, existing solutions either fall short for large formats or, for smaller formats, suffer from mediocre quality or excessive cost. These limitations prevent the current solutions from effectively addressing the demand.

Since 2014, IGN has been monitoring advancements in technology to explore a colour relief printing service for on-demand mapping, aiming to avoid the high costs associated with the thermoforming for only one exemplar. A notable French

technological innovation was introduced at the ICC 2015 in Rio de Janeiro, which enabled the production of colour relief maps, though it had height limitations. Building on this technology, IGN presents an innovative solution in this paper that addresses the height limitation and includes the first experimental results.

2. Existing Solutions for Relief Mapping

2.1 Thermoforming

Developed in 1947 by the Army Cartographic Service in Washington (Stanley, 1947), thermoforming relief mapping involves the creation of three intermediate models:

- A master model in plaster (originally aluminum), which represents the relief derived from geographical data. This model can be adjusted to refine certain areas. It cannot be used directly for thermoforming due to its insufficient strength. Nowadays, these models are typically produced using 3D printers from digital terrain models (DTMs).
- A negative of the master model, which creates the relief in hollow form.
- The final mould, created from the negative by casting a durable resin (such as epoxy), which reproduces the initial model. This mould is then perforated at multiple points to create air suction wells, allowing printed maps to be affixed to the matrix through suction.

Once the mould is produced, the production of relief maps by thermoforming can begin. For this process, the map is printed on vinyl sheets, either in large quantities using offset printing or in smaller quantities using a digital press. After the ink dries, the vinyl sheet is carefully aligned with the mould. Air is then removed from the vacuum chamber using a vacuum pump. The vacuum pulls the vinyl sheet tightly against the mould. Heat is applied to the vinyl, softening it so that it conforms to the mould under considerable force. The embossed vinyl

map is then allowed to cool in the mould while maintaining the vacuum pressure.

Due to mechanical constraints, not all relief forms can be achieved with thermoforming. For instance, large slope breaks are impractical because they would damage the vinyl sheet. These technical limitations require that the relief shapes be smoothed out on the initial mould in advance, and certain shapes may need to be excluded.

It should be noted that this process is linked to the 2D printing world. The process begins with a 2D print that is then transformed into a representation often referred to as 2.5D (a 2D surface deformed into a 3D) rather than 3D.

2.2 Additive manufacturing from the world of industry

Additive manufacturing has advanced rapidly in recent decades, with several technologies emerging to meet various needs, some of which are now accessible to individuals. Once a 3D digital model is created and adapted to the chosen printing solution, several production technologies come into play, as detailed by Barlier (2020):

- Polymerisation of a resin under the action of a laser: A resin bath is solidified layer by layer under the effect of a catalysing agent (e.g., UV laser, red actinic bulb, etc.).
- Spraying of drops of material (light-curing resin, molten wax, etc.).
- Projection of a binder onto a powder-like substrate. This family includes all processes that apply the basic process known as 3D printing. They allow printing with different colours.
- Solidification of powder under the action of a medium to high power energy source (laser or electron beam).
- Projection of powder (or wire fusion) in an energy flow (laser or plasma). Here, all the processes that produce 3D objects by depositing molten material are grouped together. They allow the fusion of many metallic materials such as stainless steels, titanium alloys, from several variants of the deposition

nozzle, the main component.

- Melting of wire through a heated nozzle. This process, the most widespread for the general public, consists of depositing molten wire through a nozzle to print in successive transverse 3D layers. This technology allows the use of thermoplastic materials, wax, but also more original materials such as chocolate.
- The assembly of layers from cut sheets or plates. This category covers processes based on materials available in sheets. These sheets can be continuous, e.g. in the form of rolls, but also discontinuous, e.g. in the form of plates of different materials, from wood to steel (Stratoconception). These additive techniques involve cutting and joining or joining and cutting of these sheets.

Hybrid additive manufacturing consists of combining at least two of its processes. The objective of these combinations is to take advantage of the different performances of the processes as well as their complementarity.

2.3 Limitations of existing additive manufacturing for relief mapping

The additive manufacturing solutions listed above are insufficient for meeting the needs of relief cartography. They fall short in several areas: insufficient size (a minimum size of 1 m² is desirable to ensure the production of maps for the IGN catalogue), printing resolution too low in powder-based solutions to consider printing writing (400 dpi minimum), low colour diversity, insufficient robustness and quality for solutions that use coloured sheet assembly, etc.

2.4 The first significant step towards printing relief maps

In 2015, at the ICC in Rio de Janeiro, IGN presented the first large size relief map obtained by 3D printing with the ACI award-winning map of Belle Ile. This relief or 2.5D printing technology, proposed by Océ, a subsidiary of the Canon group, utilized an inkjet printing

solution with the capability of adding thickness to the ink to create relief. Although Océ abandoned this printing solution in 2016, it was revived in 2020 by the startup Mihaly, founded by the French designers of the original technology who had previously worked for Océ.

This technical solution was detailed at the Time, Art & Cartography conference, held during March 16-18, 2016 at the University of Strasbourg, France. During the conference, Lecordix presented a large-format (105 cm by 135 cm) relief map of the Battle of Verdun (2016). The conference also provided an opportunity to experiment with a graphic semiology adapted for relief representation, following the manufacturing process illustrated in Figure 1.

A digital surface model is created by combining the relief data from the Digital Terrain Model (DTM) with the elevation heights assigned to various map features (such as paths, houses, and tourist points) according to choices of the relief legend. This model is then used in conjunction with a coloured raster map of the same area. The printer utilizes both files to precisely build up the relief by depositing grey ink in layers that correspond to the elevation data. At the end, CMYK inks are applied to colour the top of the relief, resulting in a colourful relief map.

The proposed technology addresses several key needs for relief mapping, including



Figure 1. Process to prepare the two raster files for relief printing of Belle Île

high printing resolution (600 dpi), large dimensions, and accurate colour reproduction. However, it faces two main challenges: the relatively high printing costs for the general public (compared to the lower prices of thermoformed maps produced in multiple copies) and, more importantly, the still limited printing heights (less than 2 to 3 cm).

3. Cartographic stratoconception

3.1 Thermoforming

In 2022, IGN proposed an innovative solution to address the issue of limited printing heights without increasing production costs.

This solution was inspired by the cardboard dog head exhibited by CIRTES company at trade fairs (Figure 2) and was realised by the patented Pack&Strat® application. This application is dedicated to 3D digital rapid packaging and uses the patented Stratoconception® rapid micro-milling process which works for materials such as wood, cardboard, foams, etc. In this process, cardboard and foam are cut using a computer-guided cutter. The dog head, which evokes the concept of contour lines, demonstrates the possibility of creating shapes without height limitations, serving as the inspiration for the innovation described below.

The process is based on a hybridisation of the previous inkjet relief printing technology existing in the world of digital plotters with the Stratoconception® technology existing in the world of 3D



Figure 2. Stratoconception® from CIRTES to make a 3D dog head with layers of cardboard.

printing, which will be detailed below.

3.2 Stratoconception® developed by CIRTES

The description of the Stratoconception® technology is described by its designer Pr. Barlier (2020) (Figure 3):

The Stratoconception® process was initiated and patented by Claude Barlier in the mid-1980s and was commercialised in 1991. This is a solid layer additive manufacturing process which consists of breaking down the CAD model of the part by calculation into a set of elementary 3D layers, called "strata", into which reinforcements and inserts are introduced. The elementary layers are put in a panoply (front/back) and manufactured in a plate material by means of rapid micro-milling, laser, water jet or cutter cutting. These thick 3D layers represent a slice very close to the original CAD model - unlike other processes which reconstruct the part from single 2D layers - they are produced directly in three dimensions by 5-axis cutting, which makes it possible to obtain ruled surfaces, or better still by 2.5-axis rapid micro-milling. In the latter case, the profile is representative of the initial 3D CAD, in terms of size, geometry and surface finish.

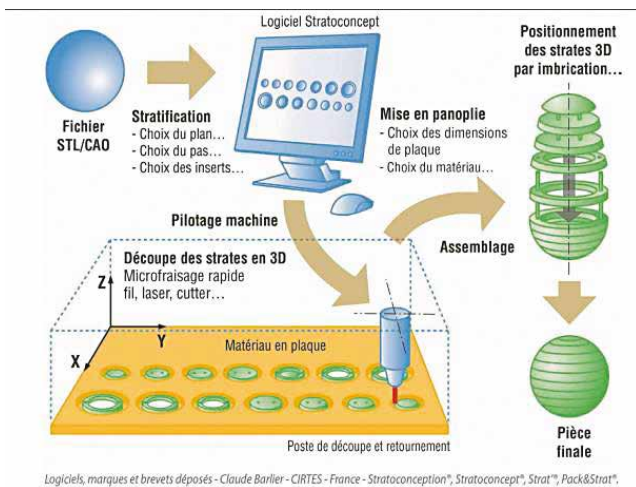


Figure 5.39 Schéma de principe de Stratoconception® (Source : CIRTES)

The layers are then positioned with inserts, or interlocked or joined with bridges to form thin-walled parts to create the final object. The final assembly can be achieved by mechanical joining, structural bonding, brazing, diffusion welding or hot isostatic pressing (HIP) depending on the material and the intended end applications. In some cases, it is possible to finish the layers after assembly by stacking (integrated into the process). The means of positioning and the type of assembly are taken into account from the moment the object is broken down, and contribute to the mechanical strength of the parts.

This solution provides a basis for creating a relief without height limitation using a strata support, to which the colour and final shape of the relief must be added.

3.3 Cartographic Stratoconception

As previously mentioned, the inkjet technology proposed by Mihaly involves applying specific ink onto a layer of support. By accumulating progressively with each scan of the surface, this ink will rise progressively to obtain the desired relief and the final layer will be carried out by inkjet in CMYK on this relief. The proposed elevation is limited to a height of 2 to 3 cm. A schematic cross-section of the printing process is provided in Figure 4.

Figure 3. Diagram of the Stratoconception® for 3D objects.

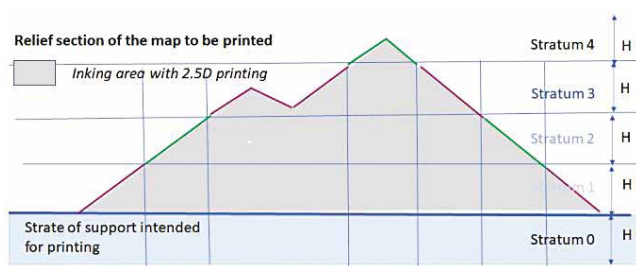


Figure 4. Schematic cross-section of the relief printing.

In the proposed innovation for relief printing, the elevation file is duplicated in two files, called even and odd layers, which will undergo similar but offset processing to bring the height of the raised print to between 0 and the thickness of the layer of the support on which the relief printing will be carried out, as shown in Figure 5. Thus, if the support used is 5 mm, the printing of any portion of the map will be between 0 and 5 mm, modulo 5 mm, to obtain the expected height of the relief map.

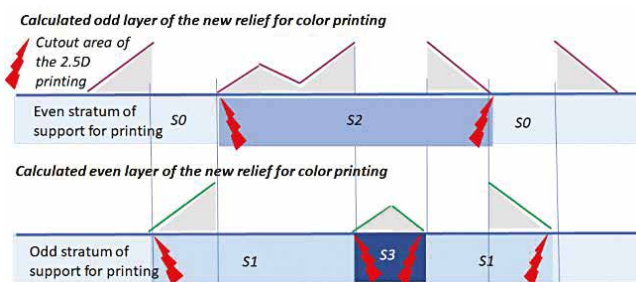


Figure 5. Schematic cross-section of the odd and even layers relief printing, with position of cutout area.

The process of cutting the even and odd numbered layers prepared as described above is applied flush with the lowest print heights (Figure 5) so that the part of the support layer N will serve as a support for the support of layer N+1 (Figure 6).

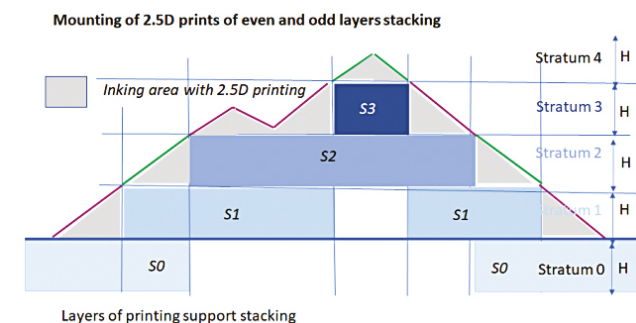


Figure 6. Schematic cross-section of odd and even layers stacking to create the relief map without height limitation.

It should be noted that the height of the support layer should not be too high for 2.5D printing to be possible with Mihaly's printer (less than 2 to 3 cm) and not too low so as not to multiply the support layers with very thin layers.

The process of cutting the even and odd numbered layers prepared as described above is applied flush with the lowest print heights (Figure 5) so that the part of the support layer N will serve as a support for the support of layer N+1 (Figure 6).

It should be noted that the height of the support layer should not be too high for 2.5D printing to be possible with Mihaly's printer (less than 2 to 3 cm) and not too low so as not to multiply the support layers with very thin layers.



Figure 7. Pre-cutting by cutter of the even layer.

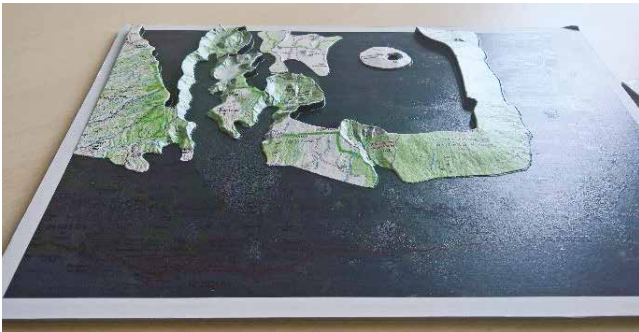


Figure 8. Printing in relief of the even layer.

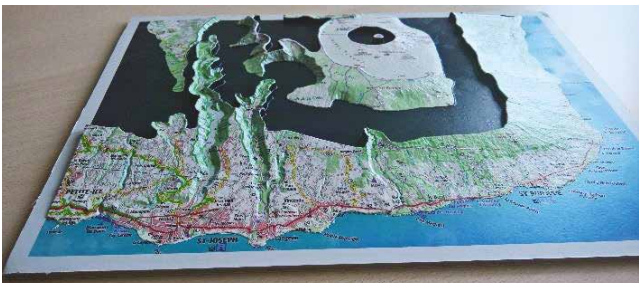


Figure 9. Printing in relief of the odd layer.



3.4 Technical choices of realization

In order to apply the principles described above, a first experiment was carried out. Several technical choices on various points were made as mentioned below.

3.4.1 The support

The support must meet different technical requirements due to the manufacturing and operating process. For the global manufacturing process, the support must be compatible with Mihaly's 2.5D inkjet printing process and with the selected cutting process of the even and odd printing layers. In addition,

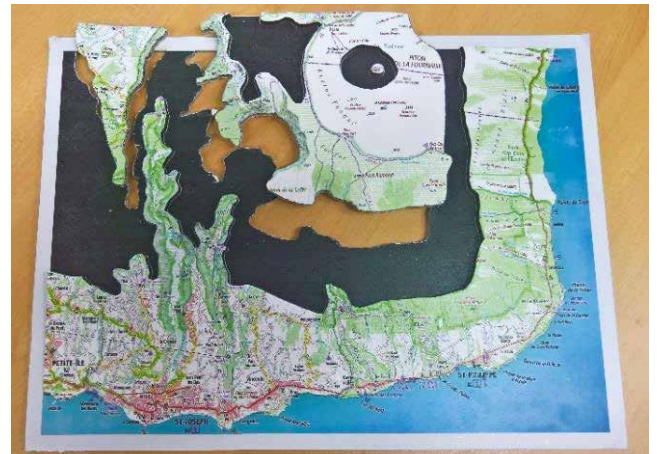


Figure 10. Separation of odd and even layers.



Figure 11. Mounting of odd and even layers stacking to create the relief map without height limitation.

the support has to meet the stability requirements for the assembly to take place and to withstand the test of time. For the first test, the KAPA® Fix foan panel in 5 mm was chosen.

3.4.2 The order of operations

Once the support has been chosen, a new technical challenge arises concerning the order of operations between printing and cutting. While it might seem logical to perform printing before cutting, this approach risks degrading the print due to the cutting process or could even render cutting impossible. The relief on the support might prevent the passage of the cutting head or the deposit of the plate in reverse.

To simplify the initial experimentation, the decision was made to first perform partial cutting, followed by printing on the pre-cut even and odd layers. It should be noted that the geometrical setting was done visually for the printing which led to some position defects. The reverse order of operations (printing with registration marks and then cutting) is currently being tested.

3.4.3 Printing

For the printing, the only solution allowing to print with heights exceeding 1 mm is the one proposed by the company Mihaly. This solution makes it possible to carry out the printing of the even and odd layers prepared upstream according to the specifications given in 2.4 (to prepare the complete relief and the colour map) and in 3.3 (to prepare the lowered relief of the even and odd layers).

3.4.4 Cutting

Many digital cutting solutions are available, each suited to different material thicknesses and types, including cutters, saws, lasers, hot wires, and water jets. However, the presence of relief ink on the support complicates the cutting process. For the first experiment, the decision was made to cut before printing, and a pre-cutting solution using a cutter was retained (see Figure 7).

It is also important to note that, depending on the chosen cutting method, technical constraints of curvature on the curve delimiting the zones to be cut out can appear.

4. First result

Following the technical choices described above, the cartographic stratoconception was implemented on a map extract of the Reunion Island. Figures 7 to 13 show the different steps to obtain the relief map without height limitation, after assembling the different cut and printed pieces in the manner of a puzzle, which fit perfectly together.

As previously mentioned, the manual setting of the printing on the pre-cut support introduced a slight shift of the printing compared to the cutting which increases locally the visualization of the connection zones.

5. Conclusion

IGN has developed and tested an innovative solution for relief printing without height limitations by hybridizing two French technologies: Stratoconception from CIRTES and color relief printing from Mihaly. The promising results from these tests suggest the potential for establishing an on-demand relief printing service, pending further testing. This solution could meet a significant existing demand from the general public.

6. References

- Barlier, C. and Bernard, A., 2020. Fabrication additive – Du prototypage rapide à l’Impression 3D, 2^{ème} édition, Ed. Dunod
- Harding C., Hasiuk F., Wood A., 2021. TouchTerrain— 3D Printable Terrain Models. In: *ISPRS International Journal of Geo-Information*, vol. 10 (3) :108. <https://doi.org/10.3390/ijgi10030108>
- Lecordix, F. 2016. Nouvelle dimension pour la sémiologie graphique. In: *Cartes & Géomatique*, Saint-Mandé, France, vol. 229-230, pp. 105-115.
- Reed, H. P., 1946. The development of terrain model in the war. In: *Geographical review*, New York, vol. 36, No.4, pp.632-652



Figure 12. Relief map after the mounting, with the layers of support stacking up.


Stanley, A. A., 1947. Plastic Relief Models. In: *The Military Engineer*, Society of American Military Engineers vol. 39, n°261, pp 287–290. <http://www.jstor.org/stable/44567205>

Sutter, F., Räber, S., Jenny, B., 2006-2017, Institute of Cartography and Geoinformation, ETH Zurich, <http://www.terrainmodels.com/contact.html>

The paper first appeared in the Proceedings of the International Cartographic Association, 5, 11, 2023.

31st International Cartographic Conference (ICC 2023), 13–18 August 2023, Cape Town, South Africa.

This contribution underwent single-blind peer review based on submitted abstracts.
<https://doi.org/10.5194/ica-proc-5-11-2023>
| © Author(s) 2023. CC BY 4.0 License.

The paper is republished with author's permission. 

US and Australia collaborate to Enhance GPS resilience

Members of the Australian Department of Defence recently joined forces with the Joint Navigation Warfare Center to put GPS devices to the test. The goal was to assess their performance under simulated jamming conditions and enhance their resilience in contested environments.

The DAGR, a widely used GPS device by both U.S. and allied forces, plays a critical role in land, sea and air navigation. By subjecting it to an anechoic chamber that mimics contested and limited GPS conditions, the team aimed to uncover insights that could enhance its resilience. www.315aw.afrc.af.mil

FCC takes important step towards new band plan

NextNav announced that the Federal Communications Commission (FCC) released a public notice seeking comment

on its innovative spectrum solution in the Lower 900 MHz band (902-928 MHz band).

On April 16, NextNav filed a rulemaking petition asking the FCC to open this proceeding to reconfigure the Lower 900 MHz band and adopt new rules to enable a terrestrial 3D PNT network to complement and back up the Global Positioning System (“GPS”). This rearrangement of the band would also free up 15 MHz of valuable low-band spectrum for 5G broadband while appropriately protecting incumbent operations.

The FCC has requested comments from the public on this proceeding that are due September 5, 2024, followed by reply comments due September 20, 2024. The Commission then considers the comments and reply comments in developing proposed rules.

NextNav is the primary geographic licensee in the Lower 900 MHz Band and has used its existing licenses to develop



4th International Conference on Environmental Management

Focal Theme: “Space for Sustainability: Bridging the Gap with Space Technology”
04 - 07 October, 2024 Hyderabad, Telangana., INDIA

Conference Themes

- Earth Observation for Environmental Sustainability
- Space Technology for Sustainable Agriculture
- Space-Based Solutions for Global Connectivity and Digital Inclusion
- Space for Sustainable Urban Planning
- AI-driven Analysis of GeoSpatial Data for Resource Optimization
- Satellite-Based Environmental Surveillance
- Digital Twins in GeoSpatial Technology for Sustainable Development
- International Collaboration for Space Sustainability
- Other Topics of Interest

Pre-Conference Workshop

Exhibition

Post Conference Field Trips

Opportunity to win best paper, best presenter and other recognitions



Organized by
CENTRE FOR ENVIRONMENT, UNIVERSITY COLLEGE OF ENGINEERING, SCIENCE AND TECHNOLOGY JAWAHARLAL NEHRU TECHNOLOGICAL UNIVERSITY HYDERABAD
Hyderabad (Telangana), 500085, India

In Association with



Venue: DST Satellite Centre for Policy Research in Geospatial Technologies for Environment and Sustainable Development, JNTU–H, Kukatpally, Hyderabad, (Telangana) India

Website: <https://icem2024jntuh.org> | Email: jntuicem2024@gmail.com, tatiparti@jntuh.ac.in

Upgrade of EU-Hydro for the Copernicus Land Monitoring Service

The Copernicus Land Monitoring Service (CLMS) framework contract for upgrading the pan-European hydrological reference dataset EU-Hydro has now kicked off. The aim with the EU-Hydro suite of products is to provide a key reference suite for hydrological applications across Europe, while also still being a reference dataset for mapping within the Copernicus services. Several new methodological approaches will be tested and implemented for its creation, with the goal of having them ready for roll-out by mid-2025.

The new EU-Hydro suite of products will be produced for all river basins in Europe. One of the main innovations will be the availability of raster layers — such as a hydrologically conditioned DEM, a flow direction map, and a flow accumulation map — derived from the state-of-the-art CopDEM 10m. Other important additions will be the topologically consistent river network, water bodies and watersheds. The upgrades will also include a newly delineated, up-to-date coastline dataset, as well as a specific layer on artificial structures of high relevance for a number of key policy areas, such as nature restoration and climate adaptation. These will include barriers and protective structures, all topologically consistent with the river network.

As a reference dataset in the CLMS portfolio, EU-Hydro provides detailed insights into water resources. It combines data from various sources — including the Copernicus Digital Elevation Model (COP-DEM) and national hydrographic datasets from Member States, as well as space-based imagery — to deliver information on the physical characteristics and geographical distribution of Europe's water bodies. pes.eu.com

industry-leading PNT expertise and products. However, much of this band is underutilized due to a legacy band plan and rules. Reconfiguring the band would pave the way for terrestrial PNT services as a complement and backup to GPS. It also would open 15 MHz of low-band spectrum for 5G broadband. <https://nextnav.com>

New IGS Analysis Center Coordinator Announced

The International GNSS Service (IGS) Governing Board and Central Bureau have announced that the next IGS Analysis Center Coordinator (ACC) will be a collaborative effort led by the NASA Goddard Space Flight Center and Geoscience Australia, with support from GFZ German Research Centre for Geosciences Potsdam and the Massachusetts Institute of Technology.

The ACC is responsible for establishing the detailed specifications for IGS products, while working closely with ACs and the IGS Reference Frame Coordinator. The new NASA/GA+ ACC will undertake a phased approach to ensure a smooth and thorough transition towards a fully multi-GNSS IGS, enhancing the accuracy and reliability of future GNSS products, while working towards achieving the IGS strategic goal of “multi-GNSS Technical Excellence.”

Lockheed Martin receives Laser Retroreflector Arrays for GPS III SV9, SV10

In partnership with NASA and the National Geospatial-Intelligence Agency, the U.S. Space Force GPS III Program Office has delivered two laser retroreflector arrays to Lockheed Martin. On May 6, the LRAs were delivered under a directed program to rapidly integrate hosted payloads on GPS satellites ahead of launch call up. The LRAs will be installed onto two GPS III satellites, SV9 and SV10, in preparation for a 2025 launch.

The addition of the LRA hosted payload onto GPS satellites marks an expansion of NASA's Space Geodesy Program space instrument network. The GPS III LRAs will allow NASA to make precise range measurements to the sub-centimeter level

using the Satellite Laser Ranging technique, enabling accurate determination of the Earth's center. The NASA Space Geodesy Program and NGA will use collected SLR data from the GPS III LRAs to maintain a globally available, high quality terrestrial reference frame.

The LRA instrument is an array of passive “Corner Cubes” that reflects laser light back to a transmitting SLR ground station. By measuring the round-trip time of the laser pulse, the ground stations are able to accurately measure the orbit of the GPS satellite. SLR can achieve millimeter-level precise orbits, which enables the scientific community to also conduct fundamental physics experiments in general relativity, as well as Earth monitoring missions, to include sea level changes, and mass redistribution in the Earth-ocean-atmosphere system.

Galileo Performance Reports for Q1 2024 are now available!

The Galileo Open Service (OS), the Galileo High Accuracy Service (HAS) and the Enhanced Search and Rescue (SAR) service performance reports for Q1 2024 are available at the European GNSS Service Centre electronic library, providing the status of the Galileo constellation and the achieved performance.

The quarterly reports provide information to users on parameters such as:

- Galileo OS: Ranging Performance, Galileo UTC and Galileo-GPS Time Offset (GGTO) Dissemination and Determination Performance, Galileo Positioning Performance, the Timely Publication of NAGUs (Notice Advisory to Galileo Users).
- Galileo HAS: Accuracy and Availability of the HAS corrections, and Service Coverage.
- SAR/Galileo Enhanced Services: Forward Link Service, Detection and Location Performance, Return Link Service, Return Link Message (RLM) Delivery Latency and Reception Probability Performance, European MEOLUT and Space Segment Availability Performance.

www.gsc-europa.eu/news/galileo-performance-reports-for-q1-2024-are-now-available

FAA makes drone history in Dallas area

In a first for U.S. aviation, the FAA has authorized multiple commercial drone operations in the same airspace. The authorizations for Zipline International and Wing Aviation allow them to deliver packages while keeping their drones safely separated using Unmanned Aircraft System Traffic Management (UTM) technology. In this system, the industry manages the airspace with rigorous FAA safety oversight.

Typically, when operating drones, the drone pilot must be able to always see the aircraft. However, new advancements in air traffic technology and procedures are providing a key step toward making these Beyond Visual Line of Sight (BVLOS) flights routine. Using UTM services, companies can share data and planned flight routes with other authorized airspace users. This allows the operators to safely organize and manage drone flights around each other in shared airspace. All flights occur below 400 feet altitude and away from any crewed aircraft.

This comes as the FAA works to release the Normalizing UAS BVLOS Notice of Proposed Rulemaking (NPRM), which would enable drone operators to expand operations while maintaining the same high level of safety as traditional aviation. We are on track to release the NPRM this year, following strong Congressional support in the recent FAA reauthorization. www.faa.gov

Wales Air Ambulance deploys Altitude Angel's Approval Services platform

Altitude Angel, a UTM (Unified Traffic Management) technology provider, has announced Wales Air Ambulance is the latest organisation to deploy its Approval Services platform allowing drone operators the ability to request and pay for operations which involve taking-off and landing from a landowner's property.

Wales Air Ambulance delivers advanced medical help to people across Wales and relies on charitable donations to raise £11.2 million every year to keep its helicopters in the air and rapid response vehicles on

the road. Every year, it's four helicopters and fleet of rapid response vehicles attend thousands of missions, covering rural countryside, towns, and cities, along the Welsh coastline and across vast mountain ranges. <https://developers.altitudeangel.com>

Saildrone fleet goes on-mission

For the fourth year, Saildrone and the National Oceanic and Atmospheric Administration (NOAA) are sailing a fleet of uncrewed surface vehicles (USVs) into hurricanes to better understand how these dangerous storms form, track, and intensify.

The mission started with 12 vehicles stationed in six operational areas identified by NOAA as having a high probability of intercepting a storm. With near-record warm ocean temperatures in the Atlantic Ocean, La Nina conditions developing in the Pacific Ocean, reduced Atlantic trade winds, and less wind shear, all of which tend to favor tropical cyclone formation, NOAA is predicted an 85% chance of an above-normal season.

Saildrone Explorer USVs are 23 feet long and carry a payload of sensors to measure air, surface, and water temperature and humidity, barometric pressure, wind speed and direction, salinity, and wave height and period. To withstand major hurricane conditions—winds over 110 mph and waves that exceed 50 feet—they have a shorter and stronger “hurricane wing,” similar to a reefed sail on a sailboat. www.saildrone.com

UAVOS gimbaled camera launched

UAVOS has launched the Gimbal 155, a new gimbaled camera purpose-built for the UAS Survey Mission program. It was designed to meet the UAV requirements for surveillance and rescue missions.

It's features include embedded video processing with electronic stabilization and object tracking, integration with external GPS/INS with real-time target location at 20 meters across multiple environments, and around 5 meters using UAVOS' Ground Control Station software. www.uavos.com

AUKUS Pillar II milestones hint at future integrated autonomous

AUKUS, the trilateral security partnership between Australia, the United Kingdom and the United States, deployed autonomous and artificial intelligence (AI)-enabled sensing systems during the Resilient and Autonomous Artificial Intelligence Technology (RAAIT) trials, showcasing advancements in their Pillar II advanced capabilities initiative.

The trials took place at multinational Project Convergence exercises hosted by the United States Army. Military personnel from the three AUKUS nations tested autonomous and AI-enabled sensing capabilities in a multi-domain battlespace—land, maritime, air, and cyber—that minimized the time between sensing enemy targets, deciding how to respond, and responding to the threat.

Once integrated into national platforms, these new sensing systems are designed to provide more reliable data, which can enable commanders to make optimal decisions and allow service members to respond more quickly to kinetic threats.

During the RAAIT exercise, a sophisticated plug-in for the Tactical Assault Kit (TAK) demonstrated impressive capabilities in enhancing military operations. This map-based software application allowed a UK RedKite UAV to dynamically detect opposing force locations by making real-time adjustments based on collected data. Simultaneously, a second UAV provided high-resolution imagery for confirmation. The integrated system seamlessly transmitted this critical information to the Tactical Operations Center (TOC), where a designated “AI officer” provided essential human oversight. Upon verification, the officer authorized an Australian XT-8 UAV to execute a simulated strike. The success of this TAK plug-in has prompted the U.S. Air Force Research Laboratory (AFRL) to plan its wider distribution, showcasing the potential for enhanced interoperability among AUKUS partners. www.defense.gov

uAvionix receiver achieves FAA TSO certification

uAvionix's ping200XR Mode S ADS-B transponder with integral aviation GPS has received technical standard order (TSO) certification from the Federal Aviation Administration (FAA). The ping200XR TSO has received TSO-C112e and TSO-C166b for transponder and ADS-B functionality – TSO-C188b for its internal pressure altimeter, and TSO-C145e for the integral aviation GPS. <https://uavionix.com>

Swift Navigation and Bad Elf Partnership

Swift Navigation recently announced its partnership with Bad Elf, a provider of GNSS receivers for GIS and survey. Through this collaboration, they will be able to deliver a complete, turnkey solution for high volume and high precision GIS data collection. www.swiftnav.com

oneNav's L5-direct safeguards defense and location services

oneNav has released the results of a test evaluating the resilience of its technology to widespread GPS interference. The testing was conducted in and around Haifa, Israel and focused on the performance of its L5-direct GPS receiver compared to GPS receivers in top smartphone and smartwatch brands.

This resilience is due to L5-direct's ability to directly acquire L5 GPS signals and bypass the L1 GPS signal, which was first invented more than 50 years ago. While current commercial GPS receivers in smartphones, car navigation systems, and airplanes can process the L5 band, they can only do so in a hybrid system that must first acquire L1. <https://onenav.ai>

U.S. Air Force extends contract with SandboxAQ

SandboxAQ has awarded a SBIR Phase 2B Tactical Funding Increase (TACFI) by the U.S. Air Force (USAF) to further develop its dual-use AQNav magnetic navigation

(MagNav) system. The funding increase will enable SandboxAQ and collaboration partner AFWERX to explore additional configurations of the core AQNav architecture.

AQNav is a breakthrough navigation technology that leverages proprietary AI Large Quantitative Models (LQMs), powerful quantum sensors, and the Earth's crustal magnetic field to provide an unjammable, un-spoofable, all-weather, day/night, terrain-agnostic, passive, real-time navigation solution for military and commercial applications, with zero reliance on GNSS. www.sandboxaq.com

GeoCue launches handheld mapping system

GeoCue has launched the TrueView GO handheld mapping system, designed for reality capture and detailed 3D mapping. It includes the 16-channel 116S and the 32-channel 132S models and integrates GNSS real-time kinematics (RTK), survey-grade lidar scanning, cameras and visual SLAM technologies. These features allow users to create real-time digital twins in indoor or outdoor environments. Geocue.com

SparkFun launches RTK evaluation kit

SparkFun Electronics has introduced its real-time kinematics (RTK) evaluation kit (EVK). It comes with a range of options for prototyping, including L1+L2 RTK GNSS, with L-Band correction built-in if needed, running on an agile processor. It features custom open-source software pre-loaded with RTK Everywhere firmware. Sparkfun.com

Leica Geosystems advances utility detection

Leica Geosystems has launched the Leica DD300 CONNECT utility locator and Leica DA300 signal transmitter, a combined, ready-to-use solution for versatile utility detection. The solution aims to enable professionals to make accurate, in-depth underground investigations and obtain on-the-spot insights regarding the underground network. leica-geosystems.com

BRINC and Echodyne to enable automated BVLOS operations

BRINC has announced a partnership with Echodyne. This collaboration will integrate Echodyne's MESA® radar technology into BRINC's purpose-built Drone as First Responder (DFR) solution. The strategic relationship enables a path toward beyond-visual line of sight (BVLOS) operations without visual observers, advanced airspace awareness for safer operations, and lowers the barrier to entry for public safety agencies looking to start or expand DFR programs.

Drone as First Responder (DFR) systems significantly lower emergency response times and enable more informed decision-making for first responders. Current FAA regulations require a visual observer onsite for drone operations to monitor flights. www.echodyne.com

Aptella partners with Sphere Drones

Aptella announces a partnership with Sphere Drones, an Australian-based full-stack technology and drone services provider. Under the agreement, Aptella



Download your copy from
www.mycoordinates.org


SUBSCRIPTION FORM

YES! I want my **Coordinates**

I would like to subscribe for (tick one)

1 year 2 years 3 years

12 issues 24 issues 36 issues
Rs.1800/US\$140 Rs.3400/US\$200 Rs.4900/US\$300

* 

First name

Last name

Designation

Organization

Address

.....

City Pincode

State Country

Phone

Fax

Email

I enclose cheque no.

drawn on

date towards subscription

charges for Coordinates magazine

in favour of 'Coordinates Media Pvt. Ltd.'

Sign Date

Mail this form with payment to:

Coordinates
A 002, Mansara Apartments
C 9, Vasundhara Enclave
Delhi 110 096, India.

If you'd like an invoice before sending your payment, you may either send us this completed subscription form or send us a request for an invoice at iwant@mycoordinates.org

* Postage and handling charges extra.

MARK YOUR CALENDAR

September 2024

Commercial UAV Expo
3 - 5 September, 2024
LAS VEGAS, USA
www.expouav.com

5th International Symposium on Engineering Geodesy
12-14 September 2024
Zagreb, Croatia
<https://sig2024.en.hgd1952.hr>

ION GNSS +
16-20 September
Baltimore, USA
<https://www.ion.org/gnss/index.cfm>

2024 GEO Symposium and Open Data & Open Knowledge Workshop
23-26 September 2024.
Hangzhou, China
<https://earthobservations.org/events>

Intergeo 2024
24-26, September
Stuttgart, Germany
<https://www.intergeo.de>

12th International FIG Workshop on the Land Administration Domain Model & 3D Land Administration
24-26 September 2024
Kuching, Malaysia
<https://gdmc.nl>

October 2024

4th International Conference on Environmental Management (ICEM 2024)
4-7 October
Hyderabad India
<https://icem2024jntuh.orgm>

Vexcel Open Day India
7-9 October, 2024
Bengaluru, India
www.vexcel-imaging.com

Romanian Surveying Week
23 - 26 October 2024
Bucharest, Romania
<https://sgr.ugr.ro>

November 2024

K-GEO Festa 2024
6-8 November
Seoul, South Korea
<https://kgeofesta.kr/fairDash.do?hl=ENG>

Trimble Dimensions
11-13, November 2024
Las Vegas, USA
www.trimble.com

45th Asian Conference on Remote Sensing
17-21 November 2024
Colombo, Sri Lanka
www.survey.gov.lk

GeoWorld
26-28 November 2024
Dubai, UAE
www.geoworldevent.com

will distribute the HubX mobile payload platform which enables autonomous scanning and mapping operations to customers across the resources, mining, construction and emergency services sectors. www.aptella.com

FlytBase and Pix4D to streamline drone data processing workflows

FlytBase and Pix4D have entered a strategic partnership, allowing FlytBase users to seamlessly upload their drone-captured data directly to the PIX4Dcloud online platform.

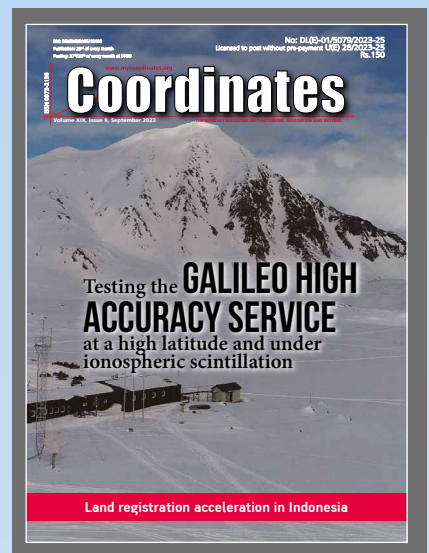
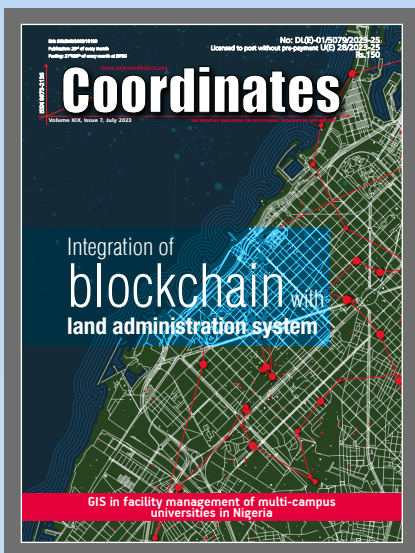
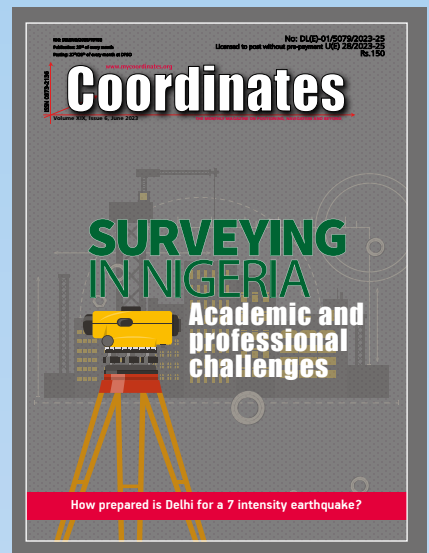
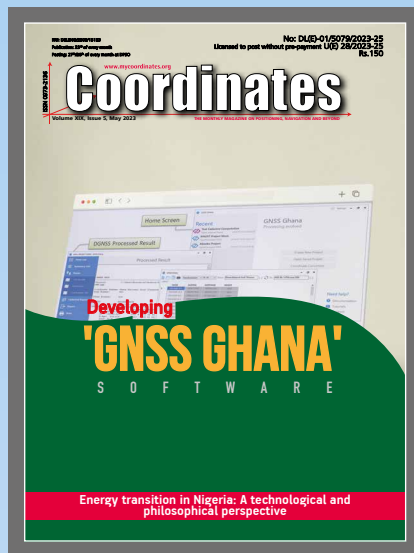
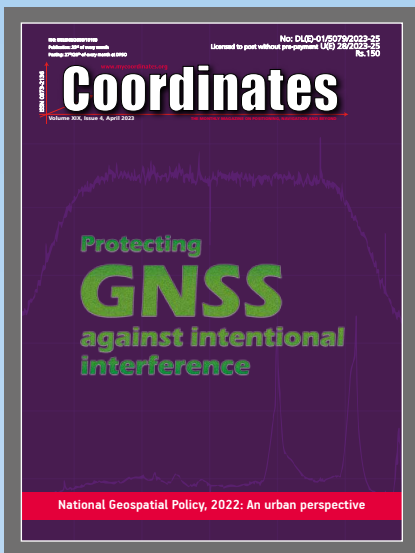
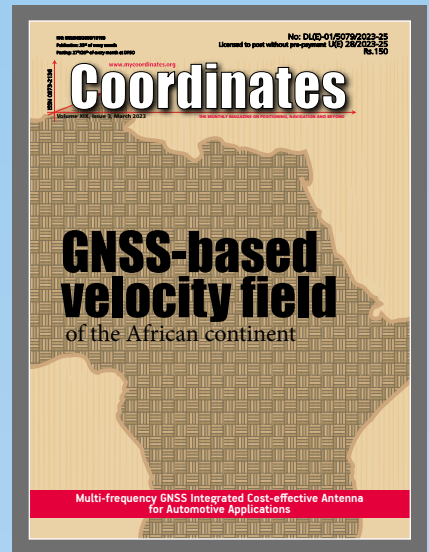
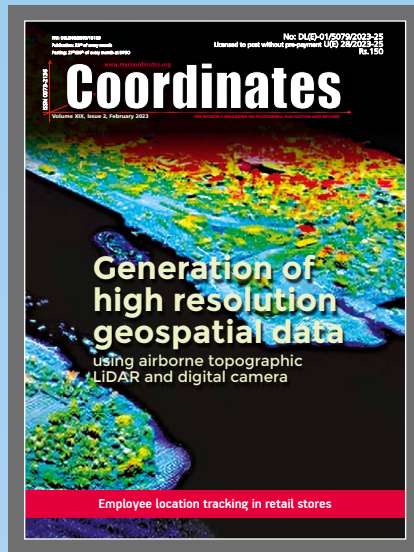
As automated UAV-docked operations become more prevalent, the volume and frequency of data collection have significantly increased. The partnership addresses this by offering users a way to conduct numerous daily missions and schedule them in advance from remote command centers. www.flytbase.com

ANELLO, Beamagine advance vehicle localization

ANELLO Photonics and Beamagine have entered a strategic partnership to enhance vehicle localization for automotive OEMs, HD mapping projects, municipalities and agricultural applications in GPS-challenged environments. This collaboration combines ANELLO's photonic gyroscopes and navigation solutions with Beamagine's lidar and vision technology to create a robust sensor fusion solution. beamagine.com

GPR, Rheinmetall Provectus advance localization technology

GPR Ground Positioning Radar has entered a strategic collaboration with Rheinmetall Provectus, a provider of autonomous navigation solutions. GPR will integrate its WaveSense localization system into Rheinmetall Provectus' autonomous platforms, enhancing positioning and navigation capabilities in GNSS-denied environments. The integration seeks to enable new capabilities such as beyond line of sight (BLOS) and GNSS-denied leader-follower operations. gpr.com



“The monthly magazine on Positioning, Navigation and Beyond”
Download your copy of Coordinates at www.mycoordinates.org



Motion & Navigation you can trust

HIGH PERFORMANCE INS/GNSS

- » High-end Technology in the Smallest Package
- » Reliable Navigation and Positioning Everywhere
- » Post-Processing with Qinertia PPK Software



Ekinox Micro

Compact INS for Mission
Critical Applications



Ellipse-D

Smallest Dual-antenna
Multi-band GNSS INS



Ellipse OEM

OEM INS when Size and
Performance Matter